Pontifícia Universidade Católica
do Rio de Janeiro

David Ronald Achanccaray Diaz

Activation of a Mobile Robot through a Brain Computer Interface based on Electroencephalographic Signal Processing

Master Dissertation

Dissertation submitted in Partial Fulfillment of the Requirements for the obtention of the Master degree to the Department of Mechanical Engineering of the PUC-Rio

Advisor: Marco Antonio Meggiolaro

Rio de Janeiro, february 2009

Pontifícia Universidade Católica
do Rio de Janeiro

David Ronald Achanccaray Diaz

Ativação de um Robô Móvel mediante uma Interface Cérebro Computador baseada no Processamento de Sinais Eletroencefalográficos

Dissertação apresentada como requisito parcial para obtenção do grau de Mestre pelo Programa de Pós-graduação em Engenharia Mecânica do Departamento de Engenharia Mecânica do Centro Técnico Cientifico da PUC-Rio. Aprovada pela Comissão abaixo assinada.

Prof. Marco Antonio Meggiolaro
Orientador
Pontifícia Universidade Católica do Rio de Janeiro

Profa. Marley Maria Bernardes Rebuzzi Vellasco
Pontifícia Universidade Católica do Rio de Janeiro

Profa. Elisabeth Costa Monteiro
Pontifícia Universidade Católica do Rio de Janeiro

Prof. José Eugenio Leal
Coordenador Setorial do Centro Técnico Cientifico – PUC-Rio

Rio de Janeiro, february 16, 2009

David Ronald Achanccaray Diaz
Graduated in Mechatronic Engineering from the UNI (Universidad Nacional de Ingenieria), Lima – Peru, in 2005. Research in Computacional Intelligence, Signal Processing, Neuroscience and Robotic.

Ficha catalográfica

Achanccaray Diaz, David Ronald

Activation of a móbile robot through a brain computer interface based on electroencephalographic signal processing / David Ronald Achanccaray Diaz ; advisor: Marco Antonio Meggiolaro. – 2009.

83 f. : il. (color.) ; 30 cm

Dissertação (Mestrado em Engenharia Mecânica)–Pontifícia Universidade Católica do Rio de Janeiro, Rio de Janeiro, 2009.

Inclui referencias bibliograficas

1. Engenharia mecânica – Teses. 2. Interface cérebro computador. 3. Eletroencefalograma. 4. Redes neurais. 5. Transformada wavelet. 6. Robótica. I. Meggiolaro, Marco Antonio. II. Pontifícia Universidade Católica do Rio de Janeiro. Departamento de Engenharia Mecânica. III. Título.

CDD: 621

To my parents Pedro and Mercedez.

Acknowledgements

To my advisor Professor Marco Antonio Meggiolaro for his patience, support and confiance dispensed during the development of this work.

To CAPES, FAPERJ and PUC-Rio, for the financial support granted, without it this work had not been possible.

To the professors members of the reviewer comission, for the suggestions that contributed to the progress of this work.

To my friends and colleagues of the PUC-Rio: Diluvina, Johanna, Gerardo, Cesar, Marko and Nilton.

Resumo

Achanccaray, David. **Ativação de um Robô Móvel mediante uma Interface Cérebro Computador baseado no Processamento de Sinais Electroencefalograficas.** Rio de Janeiro, 2009. 83p. Dissertação de Mestrado - Departamento de Engenharia Mecânica, Pontifícia Universidade Católica do Rio de Janeiro.

Este trabalho apresenta o desenvolvimento de uma interface cérebro computador como um meio de comunicação alternativo para ser utilizado na área de robótica. A dissertação contempla a implementação de um eletroencefalógrafo, alem disso, métodos e técnicas computacionais para a realização desta interface.

Para a aquisição dos sinais cerebrais se desenhou um eletroencefalógrafo, basicamente configurado por uma tripla amplificação, um filtro passa-baixos, filtros passa-altos e uma conversão analógico-digital. O processamento do sinal digitalizado é feito em duas etapas, o preprocessamento; no qual se filtra o ruído elétrico e se detecta os artefatos que possa conter o sinal. A segunda etapa é o processamento propriamente dito, na qual se faz a extração de características que definem cinco tipos de atividades mentais escolhidas segundo a especialização dos hemisférios do cérebro e referências sobre este tipo de interfaces; com as medidas obtidas se procede ao reconhecimento de padrões mediante o treinamento de uma rede neural probabilística.

O protocolo de treinamento estabelecido consta de três etapas: detecção de artifacts, classificação do tipo de atividade mental, e adaptação mutúa entre a interface e o usuário mediante a realimentação da atividade reconhecida e a atualização dos parâmetros da rede neural.

A interface desenvolvida é aplicada para a ativação de um robô móvel, associando as atividades mentais a comandos, avaliando o desempenho da interface interagindo com outros sistemas.

Palavras-chave

Interface Cérebro Computador; Eletroencefalograma; Redes Neurais; Transformada Wavelet; Robótica.

Abstract

Achanccaray, David. **Activation of a Mobile Robot through a Brain Computer Interface based on Electroencephalographic Signal Processing.** Rio de Janeiro, 2009. 83p. M.Sc. Dissertation - Departamento de Engenharia Mecânica, Pontifícia Universidade Católica do Rio de Janeiro.

This work presents the development of a brain computer interface as an alternative communication channel to be used on the robotic field. The dissertation contemplates the implementation of an electroencephalograph, the computational methods and techniques to accomplish this interface.

An electroencephalograph is designed to acquire brain signals; basically conform by a triple amplification, a low-pass filter, high-pass filters and an analog-digital converter.

The processing of the digitized signal is composed by two stages, the preprocessing; in which, the electric noise is filtered and the artifacts are detected. The second stage is the processing strictly speaking; in which, the feature extraction that define to five kinds of chosen mental activities according to the brain specialization and brain computer interface references are computed; with these measures, a probabilistic neural network is trained to classify the kind of mental activity presented.

The training protocol is defined by three stages: detection of artifacts, classification of the kind of mental activity, mutual adaptation between the user and the system through the feedback of the classified mental activity and the updating of the neural network parameters.

The brain computer interface developed is applied to activate the movements of a mobile robot, associating the mental activities to commands, evaluating the performance of the interface interacting with other systems.

Keywords

Brain Computer Interface; Electroencephalograph; Neural Networks; Wavelet Transform; Robotic.

Summary

List of figures

List of tables

List of abbreviations

AC	Altern current
ADC	Analogical-digital conversion
ALS	Amyotrophic lateral sclerosis
AS	Arithmetic operation of subtraction
BCI	Brain computer interface
CMRR	Common mode rejection ratio
CR	3D Rotation of a cube
DC	Direct current
EEG	Electroencephalography
EMG	Electromyography
ERP	Event related potentials
ERS	Event-related synchronization
ERD	event-related desynchronization
ESD	Electrostatic discharge
LM	Motor imagery of the movement of the forefinger to the left side
MA	Mental activity
MLP	Multilayer perceptron
PNN	Probabilistic neural network
P300	Positive peak at about 300 milliseconds
RAM	Random Access Memory
RF	Radiofrequency
RLD	Right-leg driver
RM	Motor imagery of the movement of the forefinger to the right side
RX	Relax
SCP	Slow cortical potentials
SNR	Signal-to-noise ratio
SSVER	Steady state visual evoked responses

1.
INTRODUCTION

1.1
Motivation

The development of interfaces between humans and machines has been an expanding field in the last decades including several interfaces using voice, vision, haptics, electromyography (EMG) signals, electroencephalography (EEG) signals and combinations between those as communication support (Garcia, 2004).

Recent studies show the possibility to analyze brainwaves to derive information about the subjects' mental state that is then mapped into some external action such as selecting a letter from a virtual keyboard or moving a robotics device. A system that utilizes these brainwaves is called Brain Computer Interface (BCI) (Millan, 2002a).

People who are partially or totally paralyzed (e.g., by amyotrophic lateral sclerosis (ALS) or brainstem stroke) or have other severe motor disabilities, can find a BCI as an alternative communication and control channel that does not depend on the brain's normal output pathway of peripheral nerves and muscles. A BCI makes it possible that these persons enhance their life quality (Wolpaw et al., 2000).

Non-invasive BCIs are based on the analysis of EEG phenomena associated with various aspects of brain function (Millan, 2002a). Thus, Birbaumer (1999) measured slow cortical potentials (SCP) over the vertex (top of the scalp). SCP are shifts in the depolarization level of the upper cortical dendrites and indicate the overall preparatory excitation level of a cortical network. Other groups look at local variations of the EEG rhythms. The most used of such rhythms are related to the imagination of movements and are recorded from the central region of the scalp overlying the sensorimotor cortex. In this respect, there are two main paradigms. Pfurtscheller's team works with event-related desynchronization (ERD) computed at fixed time intervals after the subject is commanded to imagine specific movements of the limbs (Kalcher, 1996; Obermaier et al., 2001a).

Alternatively, Wolpaw (1994) and coworkers analyze continuous changes in the amplitudes of the mu (8-12 Hz) or beta (13-28 Hz) rhythms.

Finally, in addition to motor-related rhythms, Anderson (1997) and Millán (2002b) analyze continuous variations of EEG rhythms, but not only over the sensorimotor cortex and in specific frequency bands. The reason is that a number of neurocognitive studies have found that different mental activities (such as imagination of movements, arithmetic operations, or language) activate local cortical areas at different extents. The insights gathered from these studies guide the placement of electrodes to get more relevant signals for the different tasks to be recognized. In this latter case, rather than looking for predefined EEG phenomena as in the previous paradigms, the approach aims at discovering EEG patterns embedded in the continuous EEG signal associated with different mental states.

These different BCI systems are used to operate a number of brain-actuated applications that augment people's communication capabilities, provide new forms of education and entertainment, and also enable the operation of physical devices (Millan, 2002a). The subject controls active devices by carrying out mental activities, which are associated with actions depending on the BCI application (Garcia, 2004).

BCI applications include control of the elements in a computer-rendered environment (e.g. cursor positioning (Wolpaw et al., 2000; Garcia et al., 2004), visit of a virtual apartment (Bayliss, 2001, 2003)), spelling programs (e.g. virtual keyboard (Obermaier et al, 2001b)), and command of an external device (e.g. robot (Millan & Mourino, 2003), prosthesis (Pfurtscheller et al., 2003)).

Recent applications into the robotic field are the control of a wheelchair (Bourhis et al., 2001) and the control of the robot Khepera (Millan et al., 2004); these applications could be the basis for the implementation of an external skeleton to return the total mobility of a quadriplegic person.

In this work, the hardware and the software for a BCI system is developed. The hardware for the acquisition of EEG signals is implemented in two stages; an amplification stage and an analogical-digital conversion (ADC) stage. The software of the BCI system is developed in C# language at Visual Studio 2005 environment linking developed functions in the MATLAB program for the EEG signal processing and the recognition of mental activities.

1.2 Objectives

The goal of this work is to develop an alternative unidirectional communication system between humans and robots through a BCI. To achieve this goal the following objectives must be accomplished:

- Implement a multichannel electroencephalograph.
- Develop an interface for the processing of the EEG signals.
- Integrate the BCI system to the robot to be activated.

1.3 Methodology

The development of this work consists of the following stages:

1.3.1 Implementation of an Electroencephalograph

An electroencephalograph is a device that records the brain activity through electrodes placed on the scalp. The acquisition encompasses different kinds of waves, due to the large number of interconnections of neurons and to the non-uniform structure of the brain, which depend on the position of the electrodes.

The implementation of the electroencephalograph is based on the reference "The Experimental Portable EEG/EMG Amplifier" (Benning et al., 2003), mainly in the stage of user protection, amplification and reduction of common-mode noise. The electronic design is composed of the following parts:

- Protection circuit: it protects the circuitry from electrostatic discharge (ESD) and protects the user from failing circuitry.
- Instrumental amplification: it amplifies the signal and reduces the impedance of a differential input.
- Right-Leg Driver (RLD): it raises the common-mode rejection ratio (CMRR) of the instrumentation amplifier, with a higher signal-to-noise ratio (SNR), the differential signal obtained is ensured to possess only

relevant information and a minimum of interference currents or irrelevant data.

- Amplification: it amplifies the signal amplitude to suitable levels for the analog-digital converter.
- Analog-Digital Converter (ADC): it digitalizes the signal to be processed by the computer. In this case, the data acquisition system “CompactDAQ” of the National Instruments company is used as ADC.

The amplification circuit is achieved in two stages: two high-pass first order filters are included between the amplifications, with a cutoff frequency of 0.16 Hz to remove DC-voltage offsets. The second amplification contains a low-pass second order Butterworth filter, with a cutoff frequency of 100 Hz. This reduction of the bandwidth allows getting closer the range of frequency to the brainwaves.

1.3.2 Preprocessing

The EEG signal is the endogenous brain activity measured as voltage changes at the scalp, while a perturbation is any voltage change generated by other sources. The perturbation sources include: electromagnetic interferences, eye blinks, eye movements, and muscular activity (particularly from head muscles).

The preprocessing removes external noise from EEG trials and detects the presence of artifacts. The power line noise is considered as external noise; eye blinks and eye movements are defined as ocular artifacts, while muscular activity is referred to as muscular artifact.

Electromagnetic and EEG equipment noise are narrow band pass signals. Thus, removing them through hardware or software filtering is straightforward. Typically, EEG signals are filtered in the 0.5-40 Hz frequency band; i.e. the effective EEG frequency band (Garcia, 2004).

It is worth mentioning that while in the BCI frame work they are treated as artifacts, muscular and eye movements are used as information support in other human-machine interaction systems (Barreto et al, 2000; Tecce et al., 1998); i.e. the detection of artifacts is used to interact with the system.

The power line noise is removed through notch filtering and the artifacts are detected by training of neural networks to recognize patterns obtained after the application of a wavelet transform, as discussed later in this work.

1.3.3 Processing

The signal processing is divided into two parts: feature extraction and pattern recognition.

The feature extraction consists on computing a few measurements from which it is possible to determine the different mental activity patterns. In this case, the chosen measurement is the mean of the wavelet coefficients in the principal frequency bands of the brainwaves.

Pattern recognition consists on determining an algorithm to classify the signal's features according to the corresponding mental task. A probabilistic neural network (PNN) is used as classifier, obtaining a high hit rate; the classifier must be able to recognize five different kinds of mental activities.

1.3.4 Development of the Interface

The stages of training and application of the BCI must be performed by automatic processes. The development of a graphical interface that can link all the subsystems fulfilled in different programming environments and interact with the available hardware is necessary.

The graphical interface is developed in the programming environment Visual C# adding libraries to run routines in MATLAB to control the data acquisition through the "CompactDAQ" hardware and to send commands for the mobile robot by the radiofrequency (RF) interface.

This interface offers to the user a friendly environment to develop the skill of controlling his/her brain activity, while the system can adapt to him/her.

1.3.5
Application

The validation of the BCI is made through the activation of the movements of a mobile robot, associating the mental activities to commands that can be sent to the robot by the RF interface. This application is tested with a user, evaluating the performance of the BCI with different measurements to demonstrate the accuracy and speed of the integrated system.

1.4
Outline of the Dissertation

This dissertation is divided into six chapters. This chapter serves as an introduction and overview of the work.

Chapter 2 is a description of the stages of implementation of the electroencephalograph, electronic design and fulfillment of standards.

Chapter 3 presents in detail the methods for the EEG signal preprocessing: the power line noise filtering and the procedure to detect artifacts.

Chapter 4 describes the signal processing: the algorithms for the feature extraction and the models for pattern recognition.

Chapter 5 explains the application of the BCI, to validate the integrated system and to compare the obtained performance with different users.

Chapter 6 summarizes the conclusions regarding the integration of the above methodologies. Finally, suggestions for further work are presented.

2
IMPLEMENTATION OF AN ELECTROENCEPHALOGRAPH

2.1
Introduction

In 1929, a German doctor named Hans Berger announced his discovery that it was possible to record the electrical impulses of the brain and display them graphically on paper. He also discovered that these electrical impulses changed according to the brain's activity, whether in sleep, under sedation, with lack of oxygen, and in certain neurological disorders like epilepsy. Initially, his peers laughed at him, but eventually his discovery laid the groundwork to the field that today is known as clinical neurophysiology (Griffiths et al., 2002).

An electroencephalograph is a device that records the brain activity through electrodes placed on the scalp. The acquisition encompasses different kinds of waves that depend on the position of the electrodes.

Electroencephalography has an invaluable support to the diagnostic of diseases of the central nervous system (CNS) that compromise the structure of the neurons. One of the pathologies where the electroencephalography is most useful is in the study of epilepsy, featuring unusual excitability of the neurons (Cotrina, 2003).

A first step to develop a BCI is buying or implementing the acquisition system of EEG signals. In this work, due to the high cost of an commercial electroencephalograph, an electroencephalograph of ten differential channels is designed and implemented with the suitable features to acquire EEG signals for the desired analysis.

2.2 Electroencephalography

2.2.1 Neurophysiology of the EEG

The generators of electric fields that can be registered with scalp electrodes are groups of neurons with uniformly oriented dendrites. Neurons communicate with each other by sending electrochemical signals from the synaptic terminal of one cell to the dendrites of other cells. These signals affect dendritic synapses, inducing excitatory and inhibitory post synaptic potentials (Evans & Abarbanel, 1999; Windhorst & Johansson, 1999). The EEG is a result of the summation of potentials derived from the mixture of extracellular currents generated by populations of neurons. Hereby the EEG depends on the cytoarchitectures of the neuronal populations, their connectivity, including feedback loops, and the geometries of their extracellular fields (Garcia, 2004).

The brain cortex is composed of six layers: namely molecular layer, external granular layer, external pyramidal layer, internal granular layer, internal pyramidal layer and polymorphic or multiform layer. The main physical sources of scalp potentials are the pyramidal cells of the third and fifth cortical layers (Barea, 2002).

The appearance of EEG rhythmic activity in scalp recordings results from the coordinated activation of groups of neurons, whose summed synaptic events become sufficiently large. The rhythmic activity may be generated both by neurons having the inherent capability of rhythmic oscillations, and by neurons which can not generate a rhythm on their own but can coordinate their activity through excitatory and inhibitory connections in such a manner that they constitute a network with pacemaker properties. The latter may be designated as neuronal oscillators (Windhorst & Johansson, 1999). The oscillators have their own discharge frequency, which depends on their internal connectivity. The neuronal oscillators start to act in synchrony after application of external sensory stimulation or hidden signals from internal sources, e.g. resulting from cognitive loading (Garcia, 2004).

2.2.2 EEG Rhythms

The usual classification of the main EEG rhythms based on their frequency ranges is as follows: delta (0 to 4 Hz), theta (4 to 8 Hz), alpha (8 to 13 Hz), beta (13 to 30 Hz), and gamma (higher than 30 Hz). However, this classification only partially reflects the functional variation of rhythmic activities. For example, EEG rhythms within the alpha range may be distinguished by their dynamics, place of generation and relation to certain behavioral acts (Garcia, 2004).

The alpha rhythm (Berger's wave) is typical of a resting condition and disappears when the subject perceives a sensorial signal or when he/she makes mental efforts; this rhythm is best detected with the eyes closed (Garcia, 2004; Inuso et al., 2007). It was shown that the alpha rhythm is generated by reverberating propagation of nerve impulses between cortical neuronal groups and some thalamic nuclei, interconnected by a system of excitatory and inhibitory connections and resulting in rhythmic discharges of large populations of cortical neurons (Lopes da Silva, 1991).

The beta rhythm is generated by neuronal oscillators that are located presumably inside the cortex (Lopes da Silva, 1991). The beta rhythm is typical of periods of intense activity of the nervous system and occurs mainly in the parietal and frontal regions (Garcia, 2004). Low amplitude beta with multiple and varying frequencies is often associated with active, busy or anxious thinking and active concentration. Rhythm beta with a dominant set of frequencies is associated with various pathologies and drug effects (Inuso et al., 2007).

The theta rhythm originates from interactions between cortical and hippocampal neuronal groups (Miller, 1991). It appears in periods of emotional stress or rapid eye movement during sleep (Garcia, 2004).

The delta rhythm appears during deep sleep, anesthesia, and is also present during various meditative states involving willful and conscious focus of attention in the absence of other sensory stimuli (Findji et al., 1981).

The rhythm gamma oscillations have its basis in interneuronal feedback with quarter-cycle phase lags between neurons situated close to each other in local areas of the cortex (Freeman, 1992). It is thought that gamma oscillations are associated with attention, perception and cognition.

The analysis of EEG rhythms and their interactions provide indices that are correlated with mental states such as attention (Gevins et al., 1999), memory encoding (Tallon-Boudry et al. 1998), motor imagery (Babiloni et al., 2000; Pfurtscheller et al., 2003; Wolpaw, 2000) and perception/recognition (Thorpe et al., 1996).

The range of the EEG rhythms is 5 to 100 μV peak to peak (Lee & Tan, 2006).

2.3 Implementation

The implementation of the electroencephalograph is based on the reference "The Experimental Portable EEG/EMG Amplifier" (Benning et al., 2003), mainly in the stage of user protection, amplification and reduction of common-mode noise. The electronic design is composed of the following parts.

2.3.1 Protection Circuit

The protection circuit is connected to external electrodes. It is the first stop for the EEG signal entering the amplifier box. Each channel takes two differential signals that enter the protection circuit through a pair of 2.2 k resistors and three capacitors (10pF, 100pF, 100pF), see Fig. 2.1. This initial stage suppresses RF signals that enter the system through the electrode cables. After this stage, but before the instrumentation amplifier stage, each differential signal can be observed individually. The individual signals then enter the clamping diode section. The clamping diodes are actually a pair of matched NPN and PNP transistors that begin to conduct at voltages exceeding ± 0.58V. With voltages above this level the transistors act as open circuits pulling all harmful currents down to ground (Benning et al., 2003).

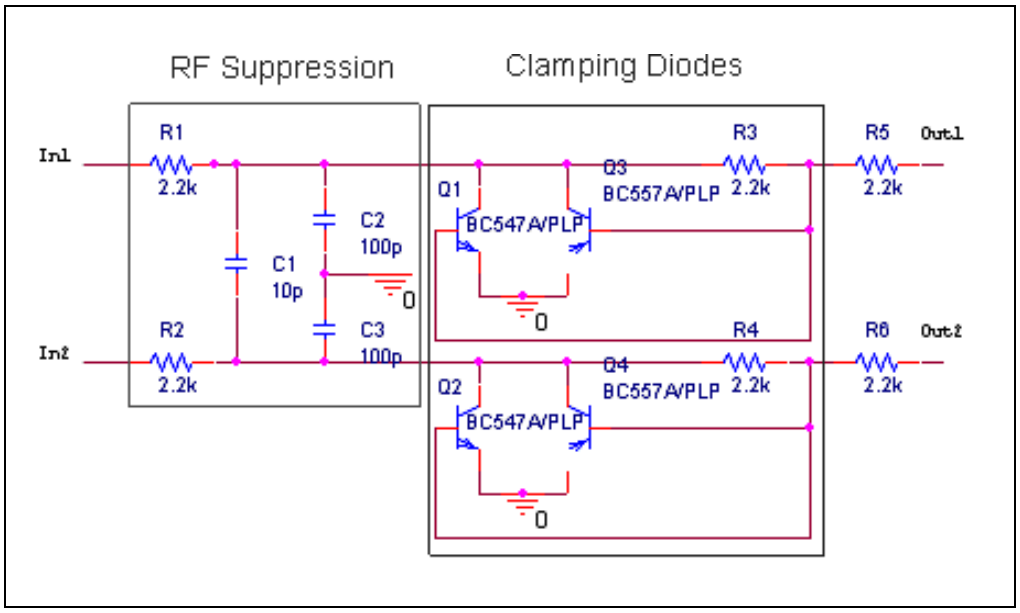

Figure 2.1 – Protection Circuit.

2.3.2 Instrumental Amplification

Instrumentation amplifiers are used to perform the crucial differential signal combination of the amplification stage. Although there are many applications and types of instrumentation amplifiers, the low-signal system has proven the most appropriate method of acquiring EEG signals (Benning et al., 2003).

The instrumentation amplifier could be considered the most important component of the EEG device. It is this stage that controls the essential combining of the differential input signals and sets up the common-mode rejection ratio for the entire device. It is also the instrumentation amplifier that must deal with the issue of noise in the incoming signal since the output signal is usually large enough to reduce this effect (Benning et al., 2003).

An instrumentation amplifier performs a combination of important tasks in the modification of an analog signal. Firstly, this amplification stage takes in two separate signals and relates them to each other. This relation is known as the differential signal. This differential signal allows for the two input signals to vary in polarity and amplitude. It also allows for the signals to possess a common DC signal that will not be introduced into the resultant output. For this reason, a

floating ground, such as it exists on the human body, is acceptable in relation to the input signals (Benning et al., 2003).

Furthermore, an instrumentation amplifier is realized through the integration of a series of three operational amplifiers (op-amp). This construction method ensures, by default, that the differential signal must be referenced to the op-amp output zero voltage. This reference now guarantees that the unknown common-mode DC signal found in the input signals is eliminated and the output is a pure differential signal related to the board ground plane (Benning et al., 2003).

It is also the job of the instrumentation amplifier to remove noise from the input signals. This concept is closely related to the previous comments about common DC signals. Over time, the human, and therefore the input signals, are subjected to variable interference currents from a variety of sources. This noise causes the floating potential of the human to randomly fluctuate up and down. Due to these fluctuations, a common-mode signal is introduced into the instrumentation amplifier, which in turn creates erroneous results to be produced at the op-amp output. There is an interesting method of counteracting this fluctuation in the form of a Right Leg Driver (Benning et al., 2003), explained in detail in the section 2.3.3.

An instrumentation amplifier consists of two variable gain op-amps and a unity gain differential amplifier. For low-signal applications, the negative inputs for the variable-gain op-amps are tied together via matching resistors, and a floating ground is created. The floating ground is actually dependent on the combined outputs of the variable gain op-amps and therefore also directly related to a known board reference ground. This floating ground allows the second stage differential amplifier to achieve CMRR values from 10 to 50dB higher than conventional instrumentation amplifier models while the two matching resistors set up the initial gain value. The variable gain op-amps act as voltage followers (due to the floating ground) and the common-mode gain equals 1. The typical instrumentation amplifier is shown in the Figure 2.2 and can be bought as an IC chip that may or may not consist of the C_f capacitors. In the figure; however, the C_f capacitors should not affect the DC component of the signal and are used to remove AC signals (Benning et al., 2003).

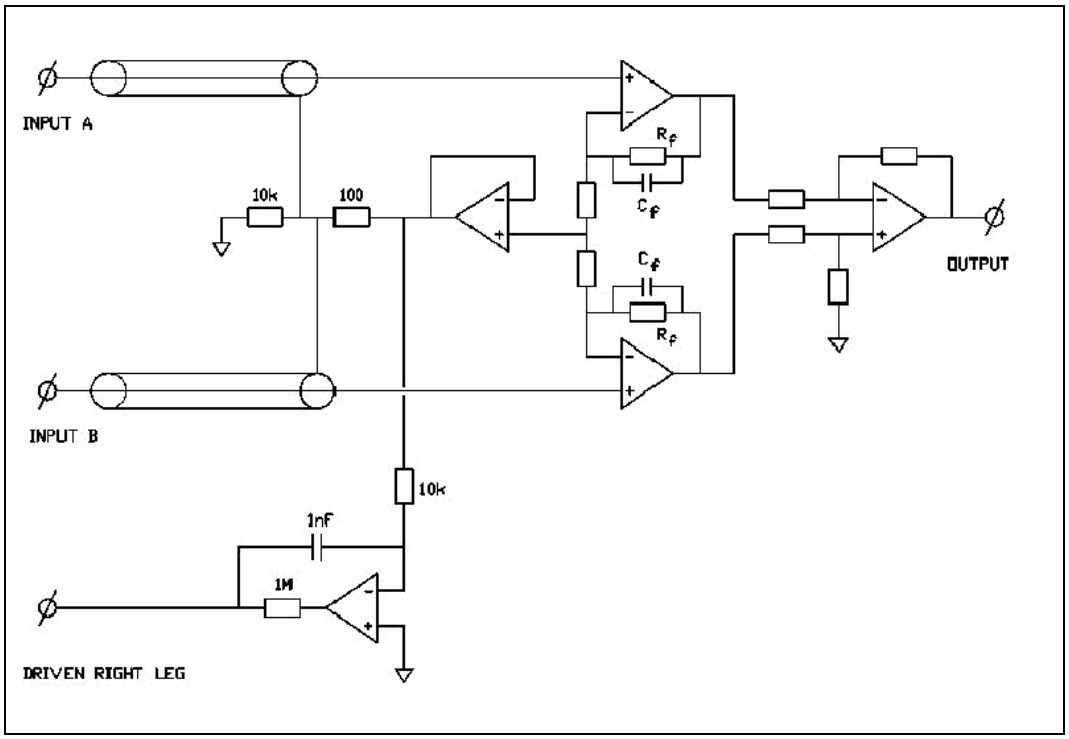

Figure 2.2 – Biomedical Instrumentation Amplifier.

The INA114 instrumentation amplifier from Texas Instruments is selected as the best circuit available for this application. The INA114 allows for the op-amp output voltage to be referenced to a variable voltage. This ensures that the differential signal will continue to remain referenced to this signal throughout the entire board and no unintentional DC offset will be obtained later in the system (Texas Instrument Incorporated, 2003).

The INA114 allows for variable gain from 1 to 10000 times to amplify the differential signal dependent on an external resistance. The variable gain G can be calculated by Eq. (1).

$$G = 1 + \frac{50k\Omega}{R_G} \tag{1}$$

where R_G is the external resistance that defines the variable gain (see Fig. 2.3). In this design $R_G = 4.4\,k\Omega$.

$$G = 1 + \frac{50k\Omega}{4.4k\Omega} = 12.36 \tag{2}$$

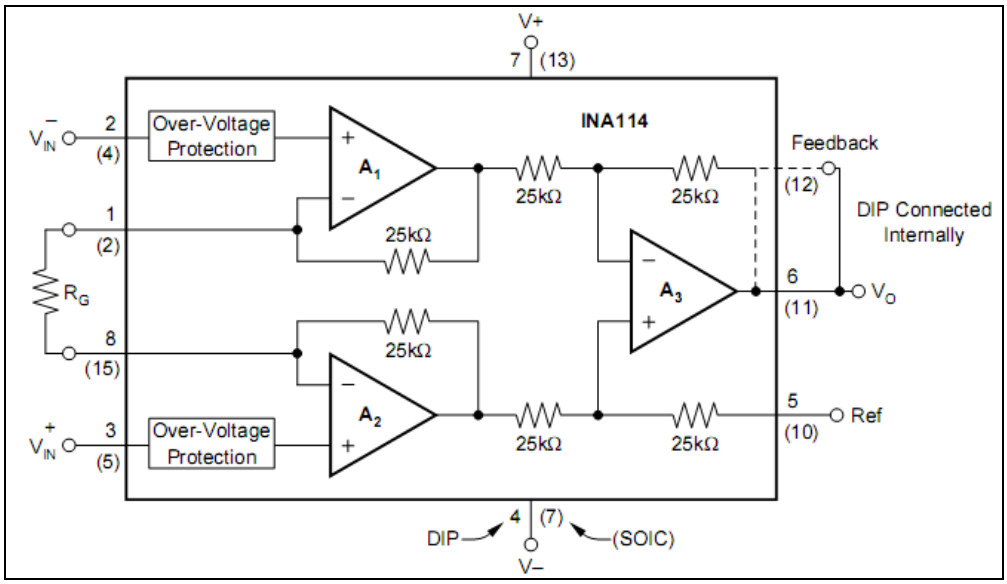

Figure 2.3 – Instrumentation Amplifier INA114 (Texas Instrument Incorporated, 2003).

2.3.3 Right-Leg Driver

The Right Leg Driver is used to raise the common-mode rejection ratio of the instrumentation amplifier. With this higher signal-to-noise ratio (SNR), the differential signal obtained is ensured to possess only relevant information and a minimum of interference currents or irrelevant data. The idea behind the RLD is to maintain a known voltage potential in the human subject that is directly related to the system board ground. This method then reduces the common-mode DC offset previously found in the system and thereby attempts to cancel any different DC offsets that individual channels or probes may experience (Benning et al., 2003).

The actual method of the RLD is quite unique. A feedback network is created, which depends on the averaged inputs from the combined instrumentation amplifier floating grounds and a GROUND signal originating from the human. This signal is then sent through an inverting gain stage that completes the feedback loop, which effectively counteracts any potential changes in the subject.

To fully understand the Right Leg Driver, it is necessary to appreciate the influences that derive its requirement. Therefore, refer to Benning et al. (2003).

This method of reducing the CMRR is actually quite common in small signal applications. In developing the INA114, Texas Instruments (TI) has actually developed its own version of a compatible RLD system as shown in Fig. 2.4.

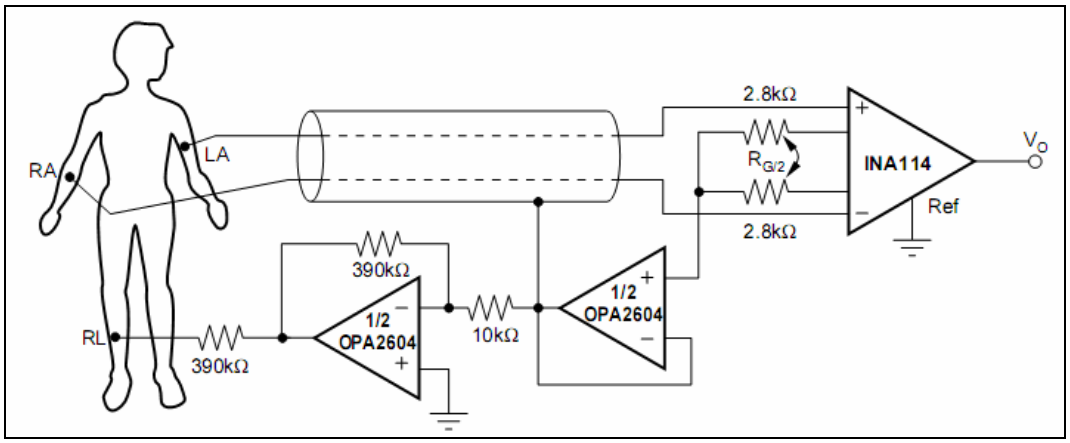

Figure 2.4 – RLD system as shown in the INA114 datasheet.

The first part of the RLD is an averaging circuit. The system presented in Fig. 2.4. has been developed by TI in an attempt to average the two negative inputs to the instrumentation amplifier and therefore balance the floating ground.

The resistor R_G usually just set up the gain of the INA114, but in RLD applications, the values are halved and utilized as shown. The RLD tap into this circuit can then be brought off this floating ground in such a way that it does not bias the amplifier with any adverse effects (Benning et al., 2003).

The next component in the circuit would be the voltage follower. The simple purpose of this op-amp is to ensure that there is no loading or feedback signal placed onto the instrumentation amplifier. Depending on which RLD model is chosen, the output of this op-amp would be where you attach any cable shielding for the electrodes. There is then a 10k resistor separating the op-amp output from the next stage (Benning et al., 2003).

The third stage of the RLD is a common carrier or averaging stage, which will be called COMM for simplicity, see Fig 2.5. All of the RLD circuits of the device are joined to this COMM line which then forces COMM to an average potential based on the various outputs of the RLD voltage followers. To this average potential (COMM) is also connected an electrode from the human which acts as a human ground reference. At this point, COMM has multiple averaged

inputs all attached to the human ground. Also, COMM is referenced to the floating ground of the instrumentation amplifier via an op-amp. In turn, the op-amp is referenced to the board ground and therefore fluctuates around some midpoint potential based on the op-amp characteristics. This combination leads to a known potential relation between the human ground and the board ground, thereby eliminating the common mode signal (Benning et al., 2003).

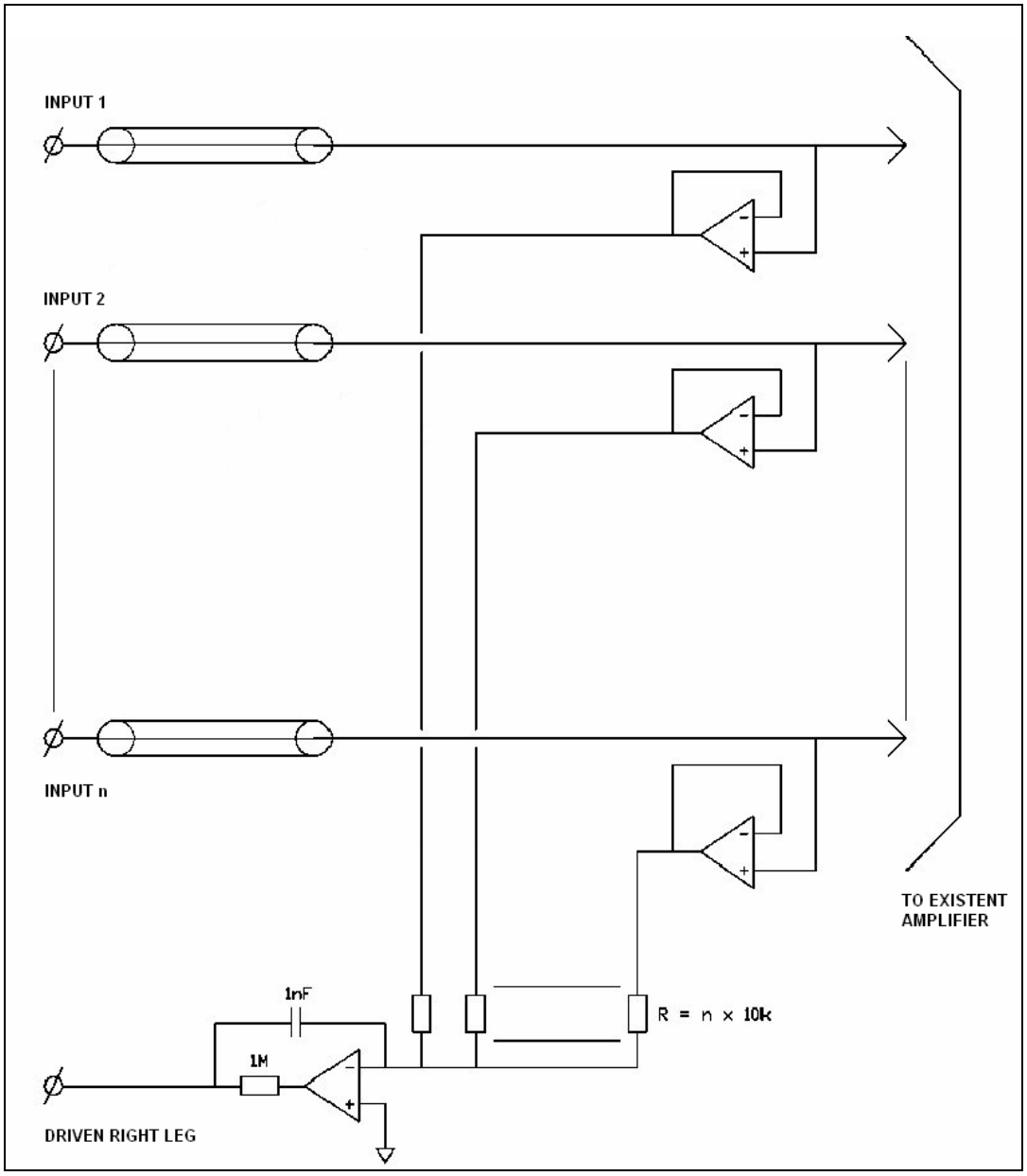

Figure 2.5 – RLD system for n-channels.

This system would be perfectly acceptable if it were not for the constant fluctuations and influence of interference currents. Due to this influence, the human ground potential varies up and down, which in turn creates variable DC offset signals and a decrease in the CMMR. In order to counteract this problem, a clever feedback loop is created that ensures a constant relation to the board ground (Benning et al., 2003).

The COMM signal is fed through the negative input of an op-amp and through a large gain stage. This high gain is necessary because the immediate influence of interference currents does not normally affect the potential of the human in the order of volts, but merely in the milli to microvolts range. The negative feedback loop therefore counteracts the influence of interference currents and ensures the stability of the human ground to that of the board ground. This assurance guarantees high CMRR values from the instrumentation amplifier (Benning et al., 2003).

2.3.4 Amplification

The amplification circuit is achieved in two stages: two high-pass first order filters are included between the amplifications, with a cutoff frequency of 0.16 Hz to remove DC-voltage offsets. The second amplification contains a low-pass second order Butterworth filter, with a cutoff frequency of 100 Hz. This bandwidth is due to the range of frequencies of the brainwaves, which is from 0 to 100 Hz.

A high-pass filter is a filter that passes high frequencies, but attenuates (reduces the amplitude of) frequencies lower than the cutoff frequency. The actual amount of attenuation for each frequency varies from filter to filter. It is useful as a filter to block any unwanted low frequency components of a complex signal while passing the higher frequencies. Of course, the meanings of 'low' and 'high' frequencies are relative to the cutoff frequency chosen by the filter designer.

The simplest electronic high-pass filter consists of a capacitor in series with the signal path in conjunction with a resistor in parallel with the signal path. The resistance times the capacitance ($R \times C$) is the time constant (τ); it is inversely

proportional to the cutoff frequency (f_C) (see Eq. (3)), at which the output power is half the input (−3 dB).

$$f_C = \frac{1}{2\pi\tau} = \frac{1}{2\pi RC} \tag{3}$$

Replacing for commercial values of capacitor and resistor, the cutoff frequency f_{C1} is obtained as

$$f_{C1} = \frac{1}{2\pi(1x10^{-6})(1000x10^{3})} = 0.1592Hz \tag{4}$$

The implementation of the high-pass filter can be seen in Fig. 2.6.

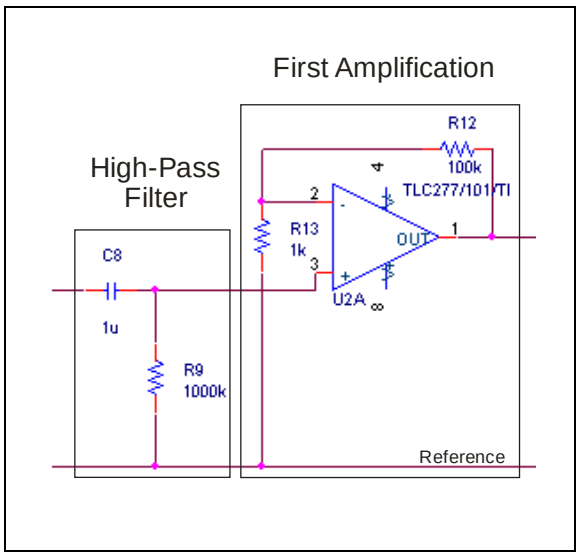

Figure 2.6 – First stage of amplification.

The first amplification stage (see Fig. 2.6) consists of a circuit with op-amp in non-inverting configuration; the amplifier gain (A_V) is obtained by the following equation (Pertence, 1988):

$$A_V = \frac{V_o}{V_i} = 1 + \frac{R_f}{R_1} \tag{5}$$

where

- V_o is the output voltage;
- V_i is the input voltage;
- R_f is the feedback resistance; and

- R_1 is the resistance connected to the negative input of the op-amp.

Replacing the values for the considered design, the amplifier gain A_{V1} is obtained as

$$A_{V1} = 1 + \frac{100x10^3}{2x10^3} = 51 \tag{6}$$

The second amplification stage includes a second order low-pass filter (see Fig 2.7).

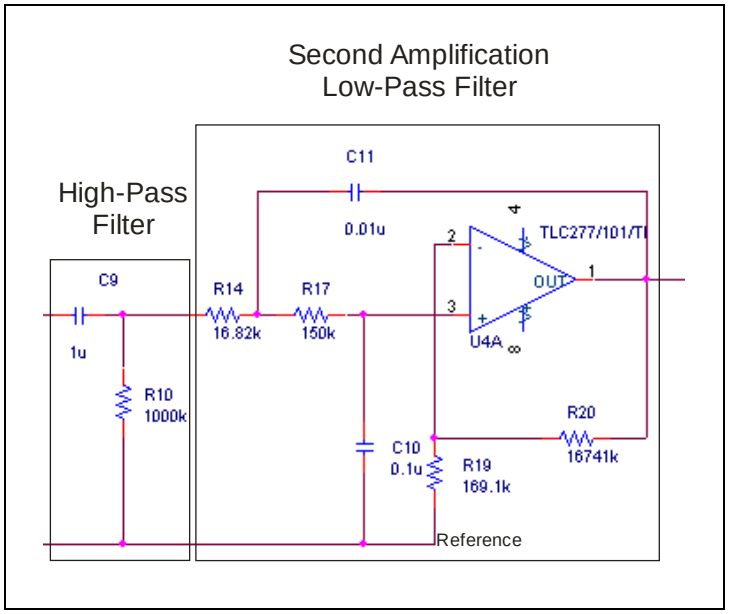

Figure 2.7 – Second stage of amplification.

The implementation of a second order filter using the structure voltage-controlled voltage-source (VCVS), a widely used circuit, can be seen in Fig. 2.8 (Pertence, 1988).

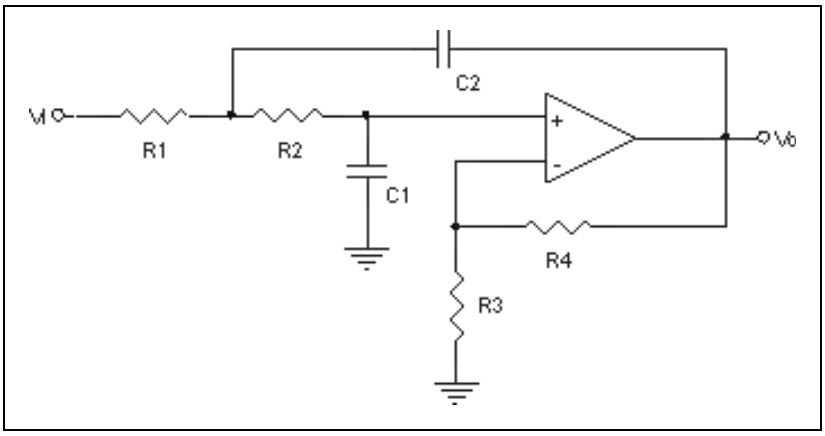

Figure 2.8 – Structure VCVS of a second order low-order filter.

The equations to implement this filter are

$$K = 1 + \frac{R_4}{R_3} \tag{7}$$

$$R_1 = \frac{2}{\left[aC_2 + \sqrt{\left[a^2 + 4b(K-1)\right]C_2{}^2 - 4bC_1C_2} \right]\omega_C} \tag{8}$$

$$R_2 = \frac{1}{bC_1C_2R_1\omega_C{}^2} \tag{9}$$

$$R_3 = \frac{K(R_1 + R_2)}{K-1} \tag{10}$$

$$R_4 = K(R_1 + R_2) \tag{11}$$

where:

- R_1, R_2, R_3, R_4 are the resistances shown in Fig. 2.8;

- C_1, C_2 are the capacitors shown in Fig. 2.8;

- K is the amplifier gain;

- a, b are obtained from the suitable tables (they define the response function or desired approximation); and

- ω_C is the cutoff frequency (f_C) in rad/s, $\omega_C = 2\pi f_C$.

After the choice of a commercial value for C_2, close to $10/f_C$, the commercial value of the C_1 must carry out the condition:

$$C_1 \leq \frac{\left[a^2 + 4b(K-1)\right]C_2}{4b} \tag{12}$$

Replacing the values for the design, $C_1 = 0.1\,\mu F$ and $C_2 = 0.01\,\mu F$ (F: Faraday); the values of a and b are obtained from Table 1 for a Butterworth second order filter and $K = 100$. The parameters calculated are the following:

$$\begin{aligned} R_1 &= 16.82k\Omega \\ R_2 &= 150.6k\Omega \\ R_3 &= 169.1k\Omega \\ R_4 &= 16.741M\Omega \end{aligned} \tag{13}$$

Table 1 – Values of the parameters a and b for the Butterworth filters, where n is a filter order.

n	a	b
2	1.414214	1
3	1.000000	1
	-	1
4	0.765367	1
	1.847759	1
5	0.618034	1
	1.618034	1
	-	1
6	0.517638	1
	1.414214	1
	1.931852	1
7	0.445042	1
	1.246980	1
	1.801938	1
	-	1
8	0.390181	1
	1.111140	1
	1.662930	1
	1.961571	1

2.3.5 Analog-Digital Converter

The analog-digital conversion is the means by which the signals are digitalized for the subsequent processing. The digitalization is carried out through the data acquisition system CompactDAQ from National Instruments; this system covers the components NI 9205 analog input module and the NI cDAQ-9172 chassis (see Fig. 2.9).

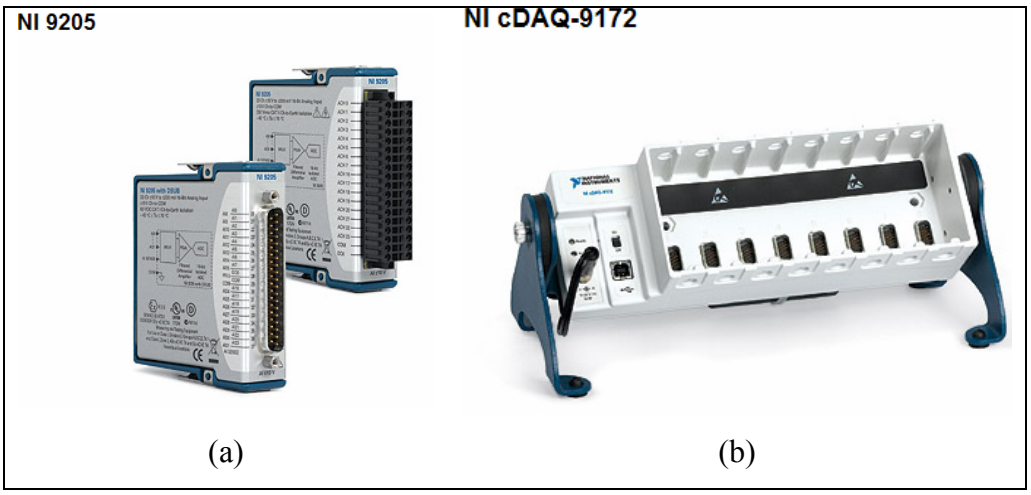

Figure 2.9 – Components of the data acquisition system CompactDAQ. (a) NI 9205 analog input module. (b) NI cDAQ-9172 chassis.

The NI 9205 also includes a channel-to-earth-ground double isolation barrier for safety, noise immunity, and high common-mode voltage range. It is rated for 1,000 Vrms transient overvoltage protection (National Instruments, 2007). The features of the NI 9205 are shown in Table 2.

Table 2 – Features of the NI 9205 analog input module.

Resolution	16 bits
Accumulated frequency rate	250 kS/s
Operation range temperature	- 40 to 70 °C
Inputs	32 single ended inputs or 16 differential inputs
Input range	±200 mV, ±1 V, ±5 V and ±10 V
Overvoltage protection	Up to 60V

The National Instruments cDAQ-9172 is an 8-slot NI CompactDAQ chassis that can hold up to eight C Series I/O modules. The chassis operates on 11 to 30 VDC and includes an AC/DC power converter. The NI cDAQ-9172 is a USB 2.0-compliant device that includes a 1.8 m USB cable.

The NI cDAQ-9172 has two 32-bit counter/timer chips built into the chassis. With a correlated digital I/O module installed in slot 5 or 6 of the chassis, one can access all the functionality of the counter/timer chip including event counting, pulse-wave generation or measurement, and quadrature encoders (National Instruments, 2007).

A graphical interface developed in Visual C# 2005 controls the data acquisition system CompactDAQ by NI cDAQ-9172, that commands the NI 9205. The amplified signals are connected to the NI 9205 for their digitalization and the cDAQ-9172 sends this information to a personal computer for processing.

2.4 Summary and Conclusions

This chapter presented theoretical fundaments of electroencephalography and details of the implementation of a ten channel electroencephalograph. The block diagram of the implemented hardware is shown in Fig. 2.10.

where

- S_i, (i = 1, 2, … 10) represents the ten electrodes used;
- M is the electrode located in the left mastoid as reference;
- RL is the electrode located in the right leg; and
- S_D is the digitalized signal.

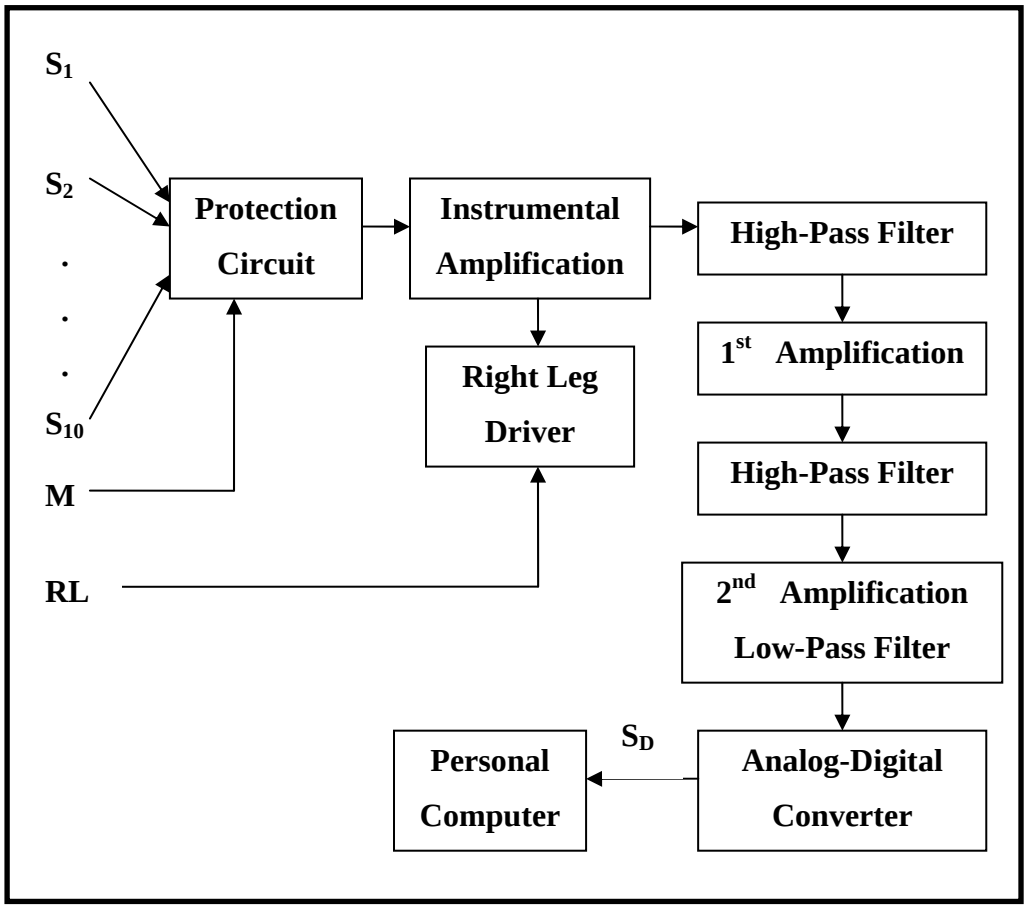

Figure 2.10 – Block diagram of the implemented electroencephalograph.

The implemented electroencephalograph is shown in Fig. 2.11, pointing out its modular parts.

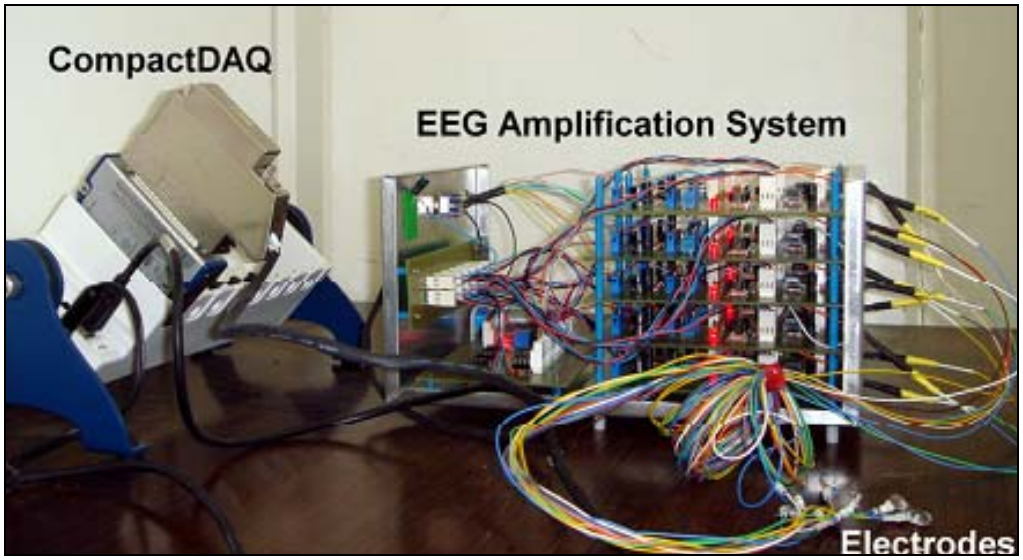

Figure 2.11 – The implemented electroencephalograph.

The overall amplification from the three stages is approximately 10^5, which generates a suitable range for the data acquisition system CompactDAQ. The electrodes position according to this system is shown in Fig. 2.12., a trial taken by the electroencephalograph in the position Fp1 of the International System 10-20 (Harner & Sannit, 1974) can be observed in Fig. 2.13.

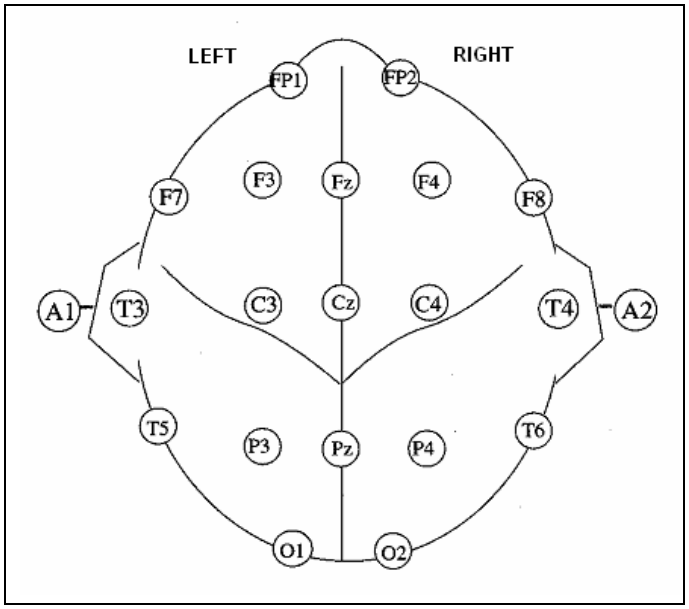

Figure 2.12 – Electrodes positions from the International System 10-20.

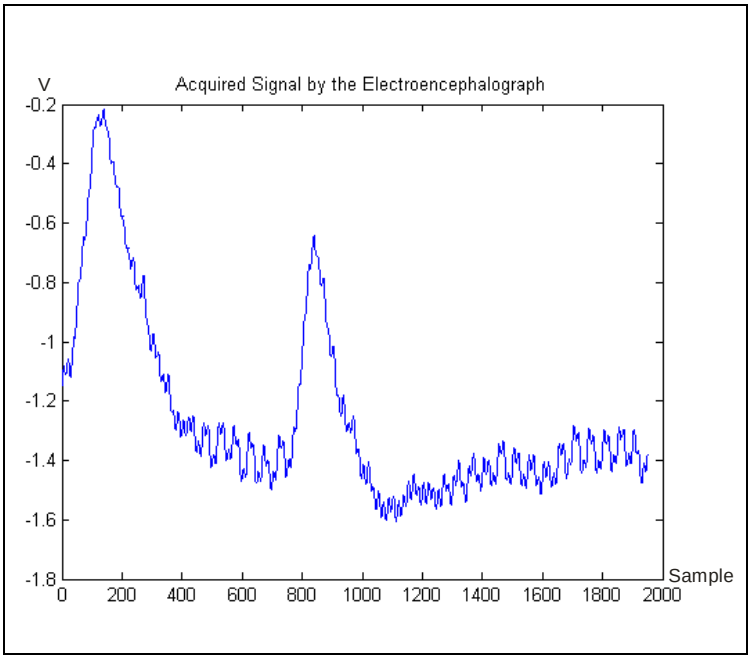

Figure 2.13 – Acquired signal in the position Fp1 of the International System 10-20.

The performance of the implemented electroencephalograph is lower than a commercial EEG, but it is enough for the desired analysis of the brainwaves and recognition of mental activities.

In the next chapter, the preprocessing steps for the EEG signal are presented.

3
PREPROCESSING

3.1
Introduction

The extraction of information from EEG data is hindered by external noise and subject-generated artifacts. Most sources of external noise can be avoided by appropriately controlling the environment in which the measurement takes place. Thus, power line noise can be easily filtered since it occupies a narrow frequency band that is located beyond the EEG band (Garcia, 2004).

Subject-generated artifacts (eye movements, eye blinks and muscular activity) can produce voltage changes of much higher amplitude than the endogenous brain activity. Even when artifacts are not correlated with tasks, they make it difficult to extract useful information from the data. In this situation the data is discarded and the subject is notified by a special action executed by the BCI. If the data containing artifacts were not discarded they could lead to misleading conclusions about the controlling performance of a subject (Garcia, 2004).

The preprocessing removes external noise from EEG trials and detects the presence of artifacts. The power line noise is considered as external noise; eye blinks and eye movements are defined as ocular artifacts, while muscular activity is referred to as muscular artifact.

As discussed before, while in the BCI frame work they are treated as artifacts, muscular and eye movements are used as information support in other human-machine interaction systems (Barreto et al, 2000; Tecce et al., 1998).

3.2
EEG Perturbations

The perturbation sources include: electromagnetic interferences, eye blinks, eye movements, and muscular activity (particularly head muscles).

Electromagnetic interferences can be avoided or at least attenuated by controlling the environment in which the measurements are carried out. Nonetheless, since the BCI setup requires to be connected to a computer, the EEG data can be corrupted by the noise from the alternate current (AC) power supplies.

These perturbations are usually well localized in frequency and located beyond the EEG band.

Eye blink artifacts are very common in EEG data. They produce low-frequency high-amplitude signals that can be much greater than EEG signals of interest. Indeed, while regular EEG amplitudes are in the range of -50 to 50 micro volts, eye blink artifacts have amplitudes up to 100 micro volts (Garcia, 2004).

Eye movement artifacts are caused by their orientation of the retinocorneal dipole. They are recognized by their quasi square shape and their amplitude in the same range of regular EEG (Overton & Shagass, 1969).

Eye blinks and eye movement artifacts (called ocular artifacts) are mainly reflected at frontal sites, e.g. electrodes Fp1 and Fp2, denominated according to the International System 10-20 (Harner & Sannit, 1974). However, they can corrupt data on all electrodes, even those at the back of the head (Garcia, 2004).

Muscular movement artifacts (muscular artifacts) can be caused by activity in different muscle groups. However, the activity in neck and facial muscles has more influence in EEG recordings. Muscular artifacts are characterized by their wide frequency content. Depending on the location of the source muscles, they can be distributed across different sets of electrodes. They mainly appear in temporal and parietal electrodes (Garcia, 2004).

3.3 Preprocessing

The preprocessing consists in applying digital filters for power line filtering and a procedure based on wavelet transforms, high order statistics and neural networks to detect artifacts.

3.3.1 Filtering

The digitized signal is filtered to guarantee that it only has frequency components in the EEG band; the used filter is the Butterworth filter, see Fig. 3.1.

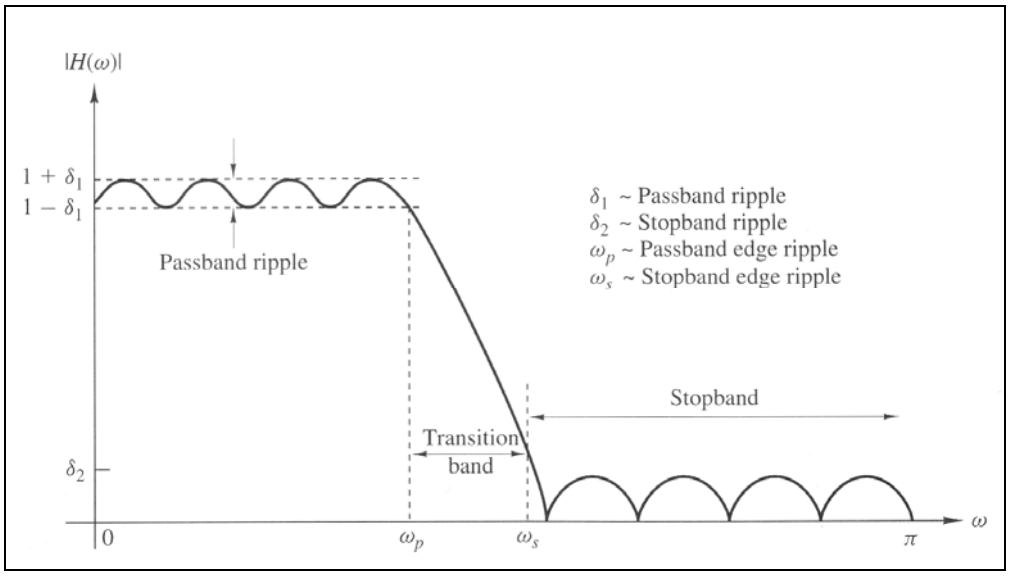

Figure 3.1 – Magnitude characteristics of physically realizable filters.

Low-pass Butterworth filters are all-pole filters characterized by the magnitude-squared frequency response.

$$\left|H(\Omega)\right|^2 = \frac{1}{1+\left(\Omega/\Omega_C\right)^{2N}} = \frac{1}{1+\varepsilon^2\left(\Omega/\Omega_P\right)^{2N}} \tag{14}$$

where

- N is the order of the filter;
- Ω_C is its -3 dB frequency (usually called the cutoff frequency);
- Ω_P is the passband edge frequency; and
- $1/(1+\varepsilon^2)$ is the bandedge value of $\left|H(\Omega)\right|^2$.

Since $\left|H(s)\right|\left|H(-s)\right|$ evaluated at s = jΩ is simply equal to $\left|H(\Omega)\right|^2$, it follows that

$$H(s)H(-s) = \frac{1}{1+\left(-s^2/\Omega_C{}^2\right)^N} \tag{15}$$

The poles of $H(s)H(-s)$ occur on a circle of radius Ω_C at equally spaced points. From Eq. (15)

$$\frac{-s^2}{\Omega_C} = (-1)^{1/N} = e^{j(2k+1)\pi/N} \qquad k = 0, 1,\ldots, \text{N-1} \tag{16}$$

and hence

$$s_k = \Omega_C e^{j\pi/2} e^{j(2k+1)\pi/2N} \qquad k = 0, 1,\ldots, \text{N-1} \tag{17}$$

The order of the filter required to meet attenuation δ_2 at a specified frequency Ω_S is easily determined from Eq. (15). Thus, at $\Omega = \Omega_S$

$$\frac{1}{1+\varepsilon^2(\Omega_S/\Omega_P)^{2N}} = {\delta_2}^2 \tag{18}$$

and hence

$$N = \frac{\log[(1/{\delta_2}^2)-1]}{2\log(\Omega_S/\Omega_C)} = \frac{\log(\delta/\varepsilon)}{\log(\Omega_S/\Omega_P)} \tag{19}$$

where, by definition, $\delta_2 = 1/\sqrt{1+\delta^2}$. Thus the Butterworth filter is completely characterized by the parameters N, δ_2, ε and the ratio Ω_S/Ω_P (Proakis & Manolakis, 1996).

The relation between Ω, ω and f is

$$\Omega = 2\pi f = \pi\omega F_S \tag{20}$$

where F_S is the sample rate.

Replacing values in Eq. (19), f_P = 30 Hz, f_S = 100 Hz, δ_1 = -3dB, δ_2 = -40dB and F_S = 1000 Hz, the required order of the filter is

$$N = 4 \tag{21}$$

The signal is filtered by a Butterworth fourth order low-pass digital filter. The magnitude and phase of the frequency response is shown in Fig. 3.2.

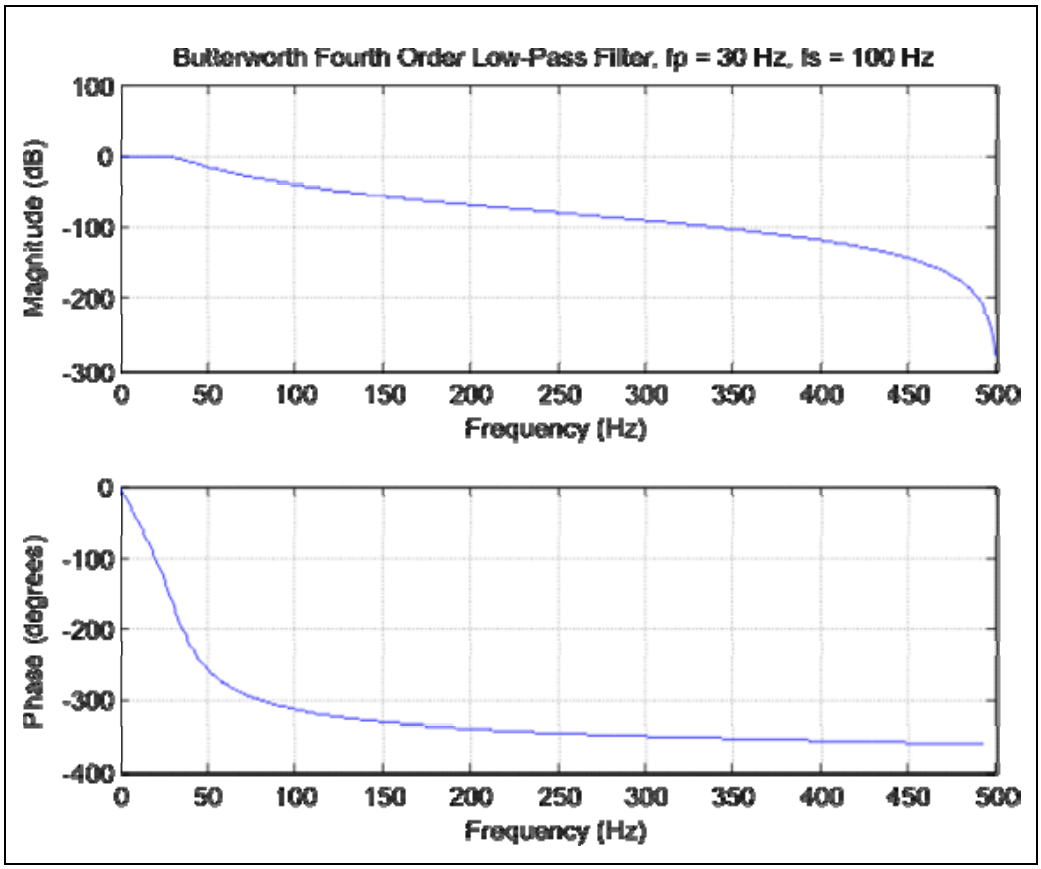

Figure 3.2 – Magnitude and phase of the frequency response of the Butterworth filter.

3.3.2 Power Line Noise Filtering

The power line noise is concentrated around a single frequency (60 Hz in Brazil) that falls beyond the EEG band. Therefore, it can be filtered using a notch filter (Hirano et al., 1974) which highly attenuates a single frequency while leaving nearby frequencies relatively unchanged. The digital notch filter z-transform is given by (Golden, 1968; Hirano et al., 1974)

$$H_n(z) = \frac{1 + a_2 - 2a_1 z^{-1} + (1 + a_2) z^{-2}}{1 - a_1 z^{-1} + a_2 z^{-2}} \tag{22}$$

where

$$a_1 = \frac{2\cos\left(\frac{2\pi f_n}{F_s}\right)}{1 + \tan\left(\frac{\pi\beta_n}{F_S}\right)} \qquad a_2 = \frac{1 - \tan\left(\frac{\pi\beta_n}{F_S}\right)}{1 + \tan\left(\frac{\pi\beta_n}{F_S}\right)} \tag{23}$$

and f_n is the notch frequency at which there is no transmission through the filter, F_S is the sampling frequency. Within the frequency band centered at f_n and of width β_n (3 dB band), all signal components are attenuated by more than 3dB, see Fig. 3.3 (Garcia, 2004).

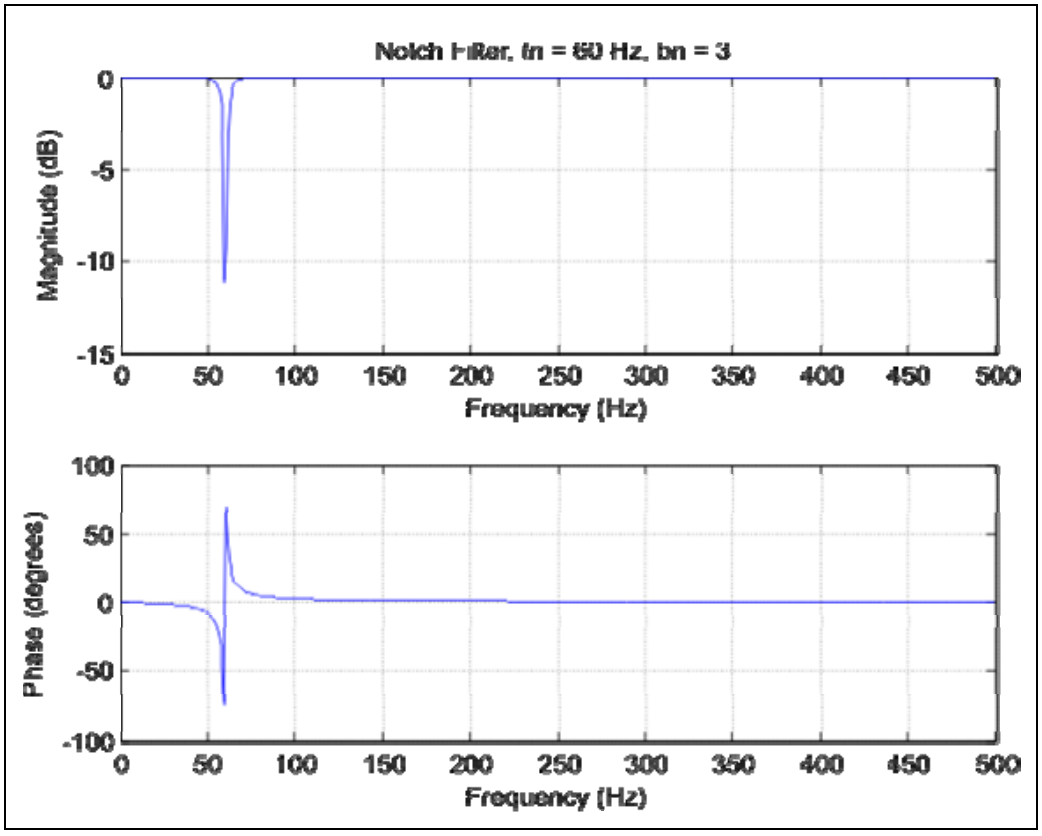

Figure 3.3 – Magnitude and phase of the frequency response of the notch filter.

For the design of the notch filter the following parameters are considered: f_n = 60 Hz and β_n = 3 Hz; replacing in Eq. (23)

$$a_1 = 1.8422$$
$$a_2 = 0.9813 \qquad (24)$$

3.3.3 Artifact Detection

The presence of eye movements, eye blinks and muscular artifacts in EEG signals can be easily detected from simple observation. As a matter of fact, each type of artifact has characteristics in time and frequency that make it distinguishable from regular EEG (Garcia, 2004).

Ocular artifacts have large amplitudes; their spectral content is mainly concentrated in the theta band and they are more prominent at frontal pole electrodes, i.e. Fp1 and Fp2 (from the International System 10-20), see Fig 2.13.

Muscular artifacts have amplitudes in the order of that of regular EEG, but their spectral content is concentrated in the beta band. These artifacts are more noticeable in central temporal and parietal electrodes, i.e. electrodes T3, T4, T5, P3, P4 and T6 (Van de Velde, 1998), see Fig 2.13.

Artifacts can be considered as singular events in the time-frequency plane that appear randomly in EEG signals. To detect the presence of artifacts in an EEG trial, the EEG signals are acquired in segments of two seconds; after the application of the filters, the wavelet transform is applied to decompose the signal frequency band to extract the EEG bands.

3.3.4 Wavelet Transform Analysis

Wavelet transforms are rapidly surfacing in fields as diverse as telecommunications and biology. Because of their suitability to analyze nonstationary signals, those whose statistical properties change over time, they have become a powerful alternative to Fourier methods in many medical applications, where such signals abound. In addition to helping in the recognition and detection of key diagnostic features, they provide a powerful means for compressing medical images with little loss of valuable information (Akay, 1997).

The familiar Fourier transform expands time-domain signals onto orthogonal basis functions (sine and cosine waves), thereby revealing the frequency content of the signals. But this method can not localize the observed frequency components in time. It is therefore best suited to describe and analyze stationary signals (Akay, 1997).

Most biomedical signals, however, do not tend to be stationary. On the contrary, they typically have highly complex time-frequency components closely spaced in time, accompanied by long-lasting, low-frequency components closely spaced in frequency. Any appropriate analysis method for dealing with them should therefore exhibit good frequency resolution with fine time resolution, the first to localize the low-frequency components, and the second to resolve the high-frequency components (Akay, 1997).

An alternative way to analyze nonstationary biomedical signals is to expand them onto basis functions created by expanding, contracting, and shifting a single prototype function, specifically selected for the signal under consideration. This wavelet method acts as a sort of mathematical microscope through which different parts of the signal may be examined by adjusting the focus. In wavelet parlance, the prototype function is known as the "analyzing wavelet" or "mother wavelet" of the signal (Akay, 1997).

Wavelet transforms can provide both very good time resolution at high frequencies and good frequency resolution at low frequencies. Interestingly, they can do so even in the absence of continuous time and frequency parameter information, thanks to the redundancies inherent in continuous wavelet signal representations. In fact, in practical applications, to reduce memory requirements and speed up numerical computation, it is usually desirable to eliminate much of this redundancy, usually by sampling the time and frequency parameters on a dyadic form (basis 2, the widely used choice) in the time-frequency plane (Akay, 1997).

Even without the efficiencies of sampling, their excellent combination of time and frequency resolution makes wavelets potentially invaluable in numerous applications, many of which fall into the realm of medical research and diagnostics. Among them, it may be found the early discovery of precursors of heart disease, studies of fetal breathing, the extraction of speech from background noise in digital hearing aids, the detection of breast cancer, and medical image compression (Akay, 1997).

The decomposition of the signal leads to a set of coefficients called wavelet coefficients. The key feature of wavelets is the time-frequency localization. It means that most of the energy of the wavelet is restricted to a finite time interval. The wavelet technique applied to the EEG signal will reveal features related to the

transient nature of the signal. All wavelet transforms can be specified in terms of a low-pass filter g, which satisfies the standard quadrature mirror filter condition

$$G(z)G(z^{-1}) + G(-z)G(-z^{-1}) = 1 \tag{25}$$

where $G(z)$ denotes the z-transform of the filter g. Its complementary high-pass filter can be defined as

$$H(z) = zG(-z^{-1}) \tag{26}$$

A sequence of filters with increasing length can be obtained

$$\begin{aligned} G_{i+1}(z) &= G(z^{2^i})G_i(z) \\ H_{i+1}(z) &= H(z^{2^i})G_i(z) \end{aligned} \qquad i = 0,...,l-1 \tag{27}$$

with the initial condition $G_0(z) = 1$. It is expressed as a two-scale relation in time domain

$$g_{i+1}(k) = [g]_{\uparrow 2^i} g_i(k), h_{i+1}(k) = [h]_{\uparrow 2^i} g_i(k) \tag{28}$$

where the subscript $[.]_{\uparrow m}$ indicates the up-sampling by a factor of m and k is the equally sampled discrete time.

The procedure of decomposition in sub-bands of the discrete wavelet transform (DWT) is schematically shown in Fig. 3.4. Each stage of this scheme consists of two digital filters and two down-samplers by 2. The first filter h[.] is the discrete mother wavelet, high-pass in nature, and the second, g[.], is its mirror version, low-pass in nature.

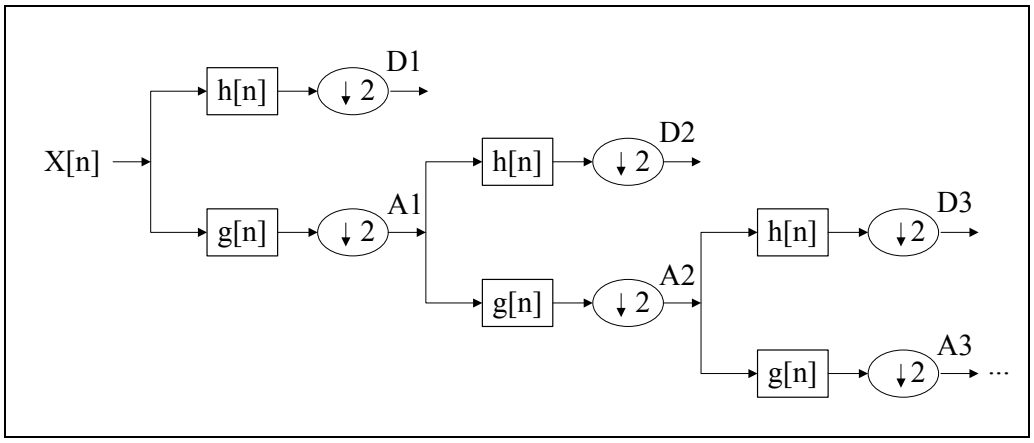

Figure 3.4 – Sub-band decomposition of DWT implementation.

The down-sampled outputs of first high-pass and low-pass filters provide the detail D1 and the approximation A1, respectively. The first approximation A1 is further decomposed and this process is continued as shown in Fig. 3.4 (Jahankhani et al., 2006).

The EEG signal is decomposed through the DWT until achieving the frequency ranges of the brainwaves; the DWT is applied in seven levels, according to Figure 3.5, in order to approximately form the four principal frequency ranges of the brainwaves:

- Delta Band [0 – 4 Hz]: (n).
- Theta Band [4 – 8 Hz]: (o).
- Alpha Band [8 – 13 Hz]: (p).
- Beta Band [13 – 30 Hz]: (q) and (k).

The sample rate (F_S) is 1000 Hz; then, the decomposition of frequency ranges begins in the range of 0 to 500 Hz.

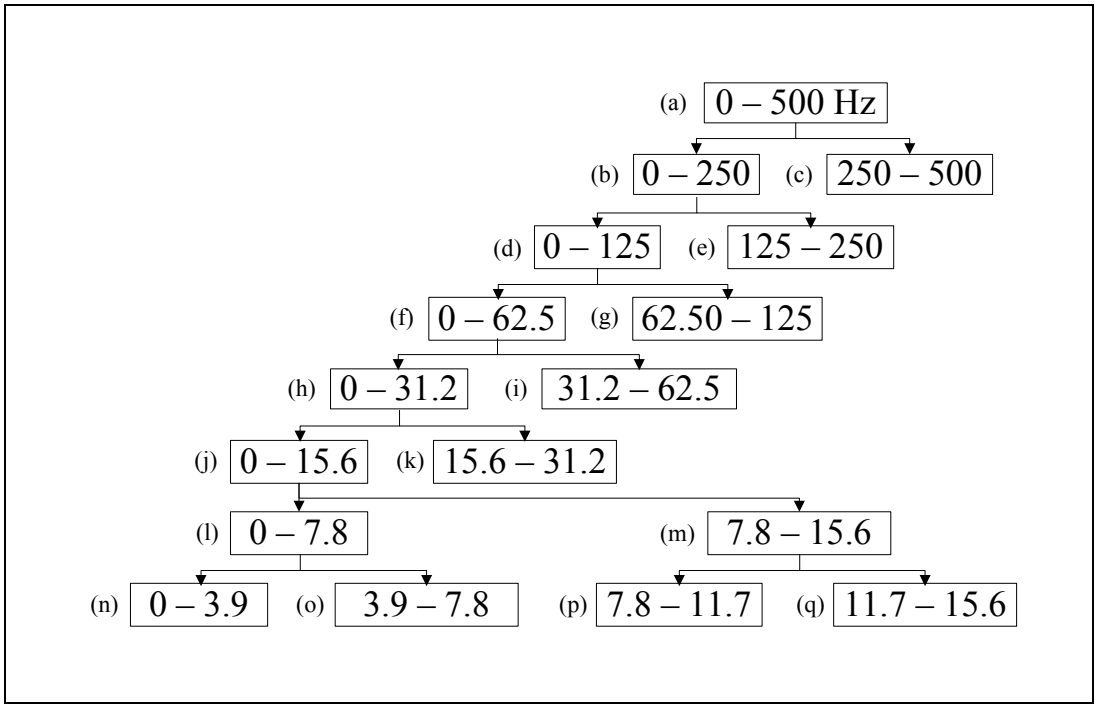

Figure 3.5 – Decomposition of the frequency ranges.

The beta and theta bands are processed to obtain their respective wavelet coefficients using the electrodes Fp1, Fp2, P3 and P4, see Fig. 3.6.

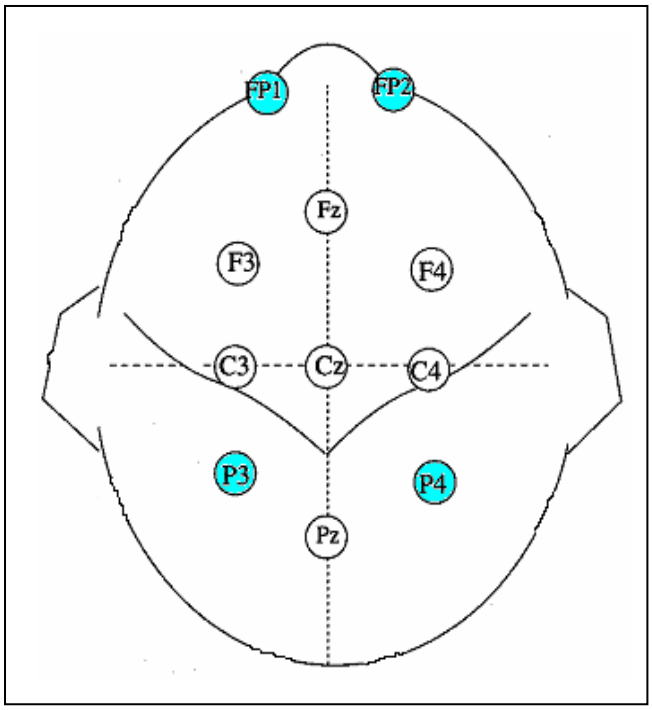

Figure 3.6 – Electrodes position according to the international system 10-20.

3.3.5 High-Order Statistics

Wavelet coefficients with artifactual activity are supposed to be "odd" with respect to other ones when an unexpected event occurs and involves its frequency range, or when it carries information about a noisy background activity. Thus, a measure of randomness might help to detect them. EEG artifacts such as eye blinks and heartbeat are typically characterized by a peaky distribution and could be detected by a measure of peakyness (Inuso et al., 2007).

The parameters that can measure the randomness and the peakyness are entropy and kurtosis, respectively (Delorme et al., 2005).

3.3.5.1 Kurtosis

Given a scalar random variable x, kurtosis (k) has the following expression:

$$k = m_4 - 3m_2^{\,2} \tag{29}$$

$$m_n = E\{(x - m_1)^n\} \tag{30}$$

where m_n is the n-order central moment of the variable and m_1 is its mean.

If the kurtosis is highly positive, the activity value distribution is highly peaked (usually around zero) with a sparse appearance of extreme values, and the identified data is likely to contain an artifact (Ghandeharion & Erfanian, 2004).

3.3.5.2 Renyi's Entropy

The definition of the Renyi's entropy is shown in Eq. (31), where α (α ≥ 1) is the order of the entropy. Equations (32-33) come from the application of the kernel estimators. The order of the entropy is set at 2, in order to equally emphasize the sub-Gaussian and the super-Gaussian components.

$$H_{R_\alpha}(X) = \frac{1}{1-\alpha}\log\sum_i P^\alpha(X = a_i) \tag{31}$$

$$H_{R_\alpha}(x) = \frac{1}{1-\alpha}\log\int_{-\infty}^{\infty} \rho_X{}^\alpha(x)dx \tag{32}$$

$$H_{R_\alpha}(X) = \frac{1}{1-\alpha}\log\{\frac{1}{N^\alpha}\sum_j[\sum_i k_\sigma(x_j - x_i)^{\alpha-1}]\} \tag{33}$$

Entropy can be interpreted as a measure of randomness.

Before computing the entropy and the kurtosis of the wavelet coefficients, they are normalized with zero-mean and unit-variance. After computing the statistic data, it is observed that a simple threshold is not enough to discriminate the occurrence of artifacts (Erdogmus et al., 2002).

Thereby, a few measurements are selected below as patterns for the training of neural networks.

3.3.6 Neural Networks

The detection system is tested with two kinds of neural networks as classifiers: multilayer perceptron (MLP) and probabilistic neural network (PNN). The detection system consists of two neural networks, joined through a logic operation OR (see Fig. 3.7).

The MLP has the ability to be an universal approximator with smaller training set requirements. It has a fast operation, ease of implementation and therefore it is the most commonly used neural network architecture. It has been

adapted to discriminate between the occurrence and the non-occurrence of artifacts. The classic gradient descending learning scheme is used here for the training of this particular network (Jahankhani, 2006).

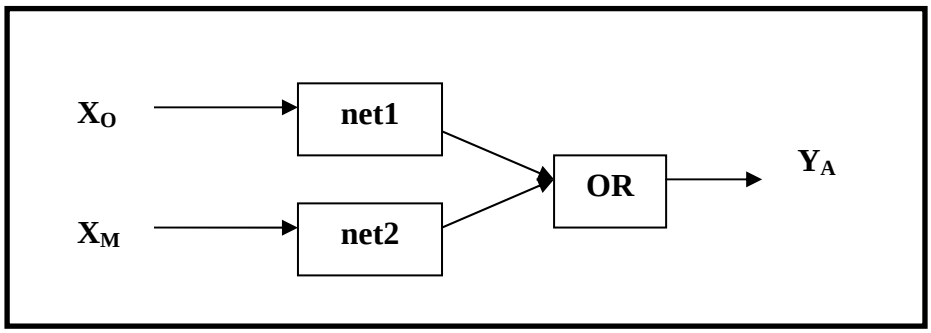

Figure 3.7 – Neural network block to detect artifacts.

The second kind of classifier is a PNN scheme. The PNN network is rapidly trained; it is usually faster than the MLP, while exhibiting none of its training pathologies such as paralysis or local minima problems (Jahankhani, 2006).

Detection of ocular artifacts is done using the wavelet coefficient kurtosis of the four electrodes (Fp1, Fp2, P3 and P4) in the frequency ranges beta (o) and theta (k), see Fig. 3.5, where X_O is a feature vector of occurrence of an ocular artifact, see Fig. 3.7.

Detection of muscular artifacts is done using the wavelet coefficient entropy and kurtosis of three electrodes (Fp1, Fp2 and P4) in the frequency range theta (k), see Figure 3.5, where X_M is a feature vector of occurrence of a muscular ocular artifact, see Fig. 3.7.

An experiment is developed to validate the procedure, considering 300 trials: 100 trials without artifacts, 100 trials with ocular artifacts, and 100 trials with muscular artifacts. The training of the neural networks is described next.

Neural network 1 (net1) is trained using 100 trials without artifacts, and 100 trials with ocular artifacts, taking 80% of the trials for the training data and 20% for the validation data.

Neural network 2 (net2) is trained in the same way, however using muscular instead of ocular artifacts.

Cross-validation is applied to determine the neural network with the better performance in the classification, the 20% of the trials for the validation data of

the networks is taken through all the samples, resulting in five possible neural networks (Haykin, 1998).

The union of the neural networks (netf) made through a logic operation OR as mentioned before, is then tested for the total of the trials. The neural networks with the better performance are chosen, the results of the tests of the neural networks are shown in Tables 3 and 4.

Table 3 – Test of the MLP neural networks (individually and united). C: Correct. I: Incorrect.

	C	**I**	**Total**	**Hit Rate (%)**
net1	35	5	40	87.5
net2	27	13	40	67.5
netf	283	17	300	94.3

Table 4 – Test of the probabilistic neural networks (individually and united). C: Correct. I: Incorrect.

	C	**I**	**Total**	**Hit Rate (%)**
net1	24	16	40	60.0
net2	27	13	40	67.5
netf	284	16	300	94.6

Tables 5 and 6 show the confusion matrices of the detection system using MLP and PNN, respectively.

Table 5 – Confusion Matrix of the Classification with MLP neural networks. S: Signal without artifact. SA: Signal with artifact.

	S	**SA**
S	87	13
SA	4	196

Table 6 – Confusion Matrix of the Classification with probabilistic neural networks. S: Signal without artifact. SA: Signal with artifact.

	S	**SA**
S	88	12
SA	4	196

The tables above show that the approach for the processing of the EEG signals and for the detection of the artifacts is suitable. The better hit rate is 94.6%, obtained by the detection system using PNN classifiers, closely followed by the hit rate using MLP classifiers, with 94.3%.

3.4 Summary and Conclusions

This chapter presented the procedure to eliminate electrical noise and to detect artifact to exclude the EEG signal or to continue the analysis.

The application of two filters, Butterworth fourth order digital filter and notch filter, guarantee the elimination of the electrical noise.

In comparison with other techniques from the literature, such as independent component analysis (ICA) (Delorme et al., 2005) were used to prepare the data of the EEG signal to discriminate the artifact occurrence. The artifacts were modeled and mixed with recorded data previously of a 32-channel EEG; applying spectral methods to isolate artifacts and standard thresholding methods on the data, detecting all trials.

The high order statistics and wavelet transform were used to determine thresholds to detect the presence of simulated artifacts (Inuso et al., 2007). The artifacts was simulated and mixed with recorded data too of a 8-channel EEG, detecting all trials.

The technique to detect artifacts uses only four electrodes Fp1, Fp2, P3 and P4, with trials of 2000 samples recorded during two seconds. The method consists in integrating high order statistics, wavelet transform and neural networks classifying a 94.6 % of the trials correctly.

The union of neural networks through a logic operation resulted in a considerable increase in performance. The specialization of the neural networks demonstrates that the system could increase even more its hit rate. Thereby, this method leaves the EEG signals free of artifacts for a more elaborated analysis.

The inconvenience of several methods used to detect artifacts is that they do not follow a pattern; therefore they can not be directly compared.

The block diagram of the preprocessing stage is shown in Fig. 3.8, where S_{WT} is the signal after the wavelet transforms.

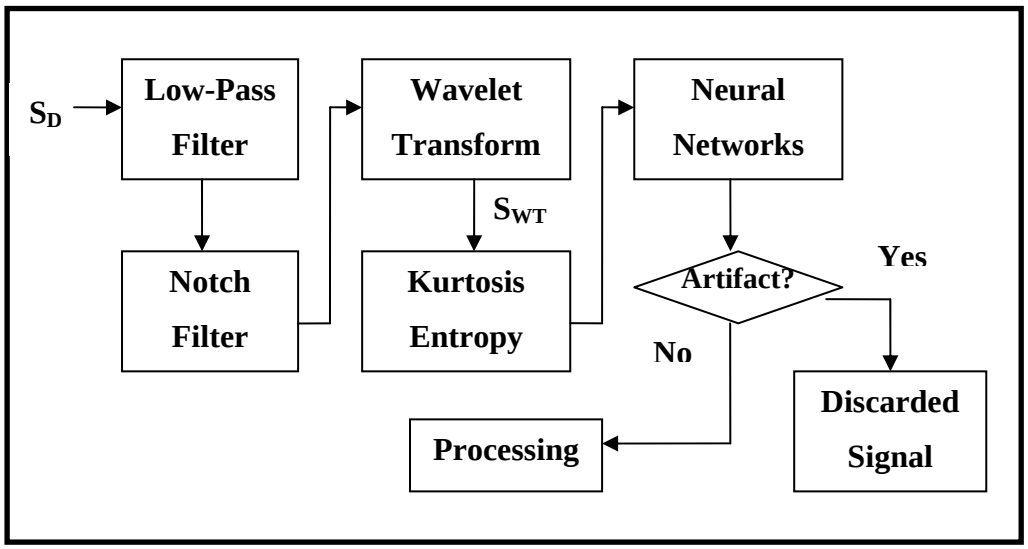

Figure 3.8 – Block diagram of the preprocessing stage.

In the next chapter, the algorithms for feature extraction and the models for pattern recognition are presented.

4
PROCESSING

4.1
Introduction

The signal processing step is divided into two parts: feature extraction and pattern recognition.

Features need to reflect properties of EEG that are relevant to the recognition of mental activities. The analysis of the generalized interaction (in time, frequency, and phase) between EEG channels has emerged as a tool to study EEG data (Garcia, 2004).

A complete analysis that takes into account time, frequency and phase would result in a very large number of features and consequently a high dimensional feature vector. Because of the particular requirements of BCI applications, according to which a continuous adaptation of the recognition models and a reasonable training time are required, high dimensional feature vectors are clearly non-suitable (Garcia, 2004).

There is a large consensus that an efficient and practical BCI should exhibit the following properties: high scores of correct recognition and rapid responses, on the order of a second, to increase the bit rate of the communication channel (Millan, 2002b). The accuracy of the classifier is fundamental for a correct recognition.

Several classifiers are mentioned in (Garcia, 2004), such as optimal Bayesian classifier, vector quantization, distance sensitive vector quantization (a variant of vector quantization in which the distance takes into account the discriminative power of each feature), multi-layer neural networks (deal with general separation boundaries between the sets of mental tasks), auto-associative neural networks (which are able to directly operate in the time domain, the feature extraction procedure is therefore no longer necessary) (Devulapalli, 1996), linear and nonlinear classifiers are compared in Muller et al., 2003 for BCI applications.

Other approaches include logistic regression classifiers, hidden Markov models and microstate decomposition (Pascual-Marqui et al., 1995) to classify sequences of features, and Bayesian time series classification (Sykacek et al., 2003).

Machine learning state-of-the-art kernel methods such as support vector machines and kernel novelty detection algorithms are mentioned in Garcia et al., 2003.

4.2 Mental Activities

The mental activities used in current BCIs are chosen in accordance with brain hemispheric specialization studies, which suggest that the two hemispheres of the human brain are specialized for different cognitive functions. In particular, the left hemisphere appears to be predominantly involved in verbal and other analytical functions and the right one in spatial and holistic processing (Allanson, 2000; Galin & Ornstein, 1975). Thus, typical mental activities (MA) include: evoked responses to external stimuli, imagined limb movement, and spatial, geometrical, arithmetical and verbal operations.

BCIs can be categorized by the type of mental activities: there are BCIs based on Evoked Response or Operant Conditioning. In the first, the subject's reaction to stimuli is monitored. Such BCI is the most common due to its implementation simplicity; however, it is limited because it depends on specific abilities from the subject such as gaze direction control, which might be a problem with handicapped patients. The second type, on the other hand, monitors directly the subject's behavior, without the need for external stimuli and the ability to detect them. Both types are presented next.

4.2.1 Evoked Response based BCIs

Evoked responses are related to cognitive methods in psychology (Utall, 1999; Vaughan et al., 2003) which consider the mind as an information processing device whose output depends on the relationship between stimuli and the activation of cognitive processes.

External visual or auditory events (e.g. blinking objects on a computer screen, flashing elements on a grid or brief sounds) elicit transient signals in the EEG that are characterized by voltage deviations known as event related potentials (ERP). When the subject pays attention to a particular stimulus, an ERP that is time locked with that stimulus appears in his/her EEG. The changes in the EEG signals induced by the ERP can be detected by using averaging or blind source separation methods (Huggins et al., 1999; Makeig et al., 1997). If actions are associated with stimuli, the subject can gain control of the BCI by focusing his/her attention on the stimulus corresponding to the desired action.

Examples of BCIs functioning under evoked conditions are those using the P300 and the steady state visual evoked responses (SSVER), as described next.

Infrequent or particularly significant auditory, visual, or somatosensory stimuli, when mixed with frequent or routine stimuli, typically evoke in the EEG over the parietal cortex a positive peak at about 300 (P300) milliseconds after the stimulus presentation (Donchin & Smith, 1970; Donchin et al., 2000; Farwell & Donchin, 1998; Sutton et al., 1965; Walter et al., 1964).

Flicker stimuli of variable frequency (2-90Hz) elicit a steady state visual evoked response in the EEG which is characterized by an oscillation at the same frequency as the stimulus. Thus, an SSVER can be detected by examining the spectral content of the signals recorded in the visual region, namely electrodes O1 and O2 of the International System 10-20 (Harner & Sannit, 1974).

When actions are associated with targets flickering with different frequencies, the subject can control the BCI by gazing at the target corresponding to the desired action (Calhoun et al., 1997; Cheng et al., 2002; Gao et al., 2003; Middendorf et al., 2000). BCIs based on this principle depend on the subject's ability to control gaze direction.

4.2.2
Operant Conditioning based BCIs

Operant conditioning is related to behavioral methods in psychology (Skinner, 1938; Vaughan et al., 2003). According to them, the subject can acquire control skills through adequate feedback (operant conditioning feedback).

Effective attempts to provide control through operant conditioning feedback begun in the 1950's when some clinicians used the so-called neurofeedback to treat people suffering from attention deficit, hyperactivity, depression and even epilepsy. Based on the principle that functions of the autonomous and central nervous systems can be retrained for better adaptive functioning, neurofeedback practitioners trained their patients to self-regulate their brain activity through operant feedback. In some cases, they obtained astonishing results (Robbins, 2000).

Examples of BCIs functioning under operant conditioning use slow cortical potential shifts (SCPS), oscillatory sensorimotor activity, and other hemispheric specialized mental activities.

SCPSs last from a few hundred milliseconds up to several seconds and indicate the overall preparatory excitation level of a cortical network. They are universally present in the human brain. Negative SCPSs are typically associated with movement and other functions involving cortical activation, while positive SCPSs are usually associated with reduced cortical activation (Birbaumer et al., 2000; Rockstroh et al., 1984).

Subjects can learn through operant feedback to produce a SCPS in an electrically positive or negative direction for binary control (Birbaumer et al., 2000; Perelmouter & Birbaumer, 2000). This skill can be acquired if the subjects are provided with a feedback on the course of their SCPS production and if they are positively reinforced for correct responses (Birbaumer et al., 2003).

In oscillatory sensorimotor activity, populations of neurons can form complex networks which are at the origin of oscillatory activity. In general, the frequency of such oscillations decreases with an increase in the number of synchronized neuronal assemblies (Singer, 1993). Two types of oscillations are especially important: the Rolandic mu rhythm, in the range from 7 to 13 Hz, and the central beta rhythm, above 13 Hz, both originating in the sensorimotor cortex (Jasper & Penfield). Sensory stimulation, motor behavior, and mental imagery can change the functional connectivity within the cortex and result in amplitude suppression (event-related desynchronization (ERD)) or in an amplitude enhancement (event-related synchronization (ERS)) of mu and central beta rhythms (Pfurtscheller & Aranibar, 1977).

Preparation and planning of self-paced hand movement results in a short-lasting desynchronization (ERD) of Rolandic mu and central beta rhythms. Electrocorticographic recordings exhibit ERD in the alpha band associated with hand and foot movement. The general finding is that, similarly to the mu rhythm (around 10 Hz), beta oscillations desynchronize during the preparation and execution of a motor act (Pfurtscheller & Neuper, 2001).

Motor imagery may be seen as mental rehearsal of a motor act without any overt motor output. It is broadly accepted that mental imagination of movements involves brain regions/functions similar to that involved in programming and preparing such movements (Jeannerod, 1995).

In addition to imagined motor tasks, other mental activities for which evidence for hemispheric specialization was found are: geometrical MA (Nikolaev & Anokhin, 1998) (e.g. imagination of a geometric 3D object and the rotation of such an object), verbal MA (Galin & Ornstein, 1972; Koenig et al., 1998) (e.g. mental composition of a letter) and arithmetic MA (Rotenberg & Arshavsky, 1997) (e.g. mental counting, multiplication, etc.). Few research groups considered these mental activities for BCI applications. Hemispheric specialized mental activities open the possibility to implement more control capabilities and in certain cases they are easier to perform than imagined motor mental activities (Garcia, 2004).

Since they are able to extend the control capabilities beyond binary commands, motor imagery and hemispheric specialized mental activities are used in this work.

4.3
Feature Extraction

The BCI developed in this work is based in operant conditioning. The mental activities defined are the motor imagery of the forefinger movement of the right hand to the right and to the left side, imagination of the 3D rotation of a cube, arithmetic operation of subtraction by a constant number and the mental state of relax.

After the application of the wavelet transform, the wavelet coefficients contain useful information in the time and frequency domain. The next step is the feature extraction, which consists on computing a few measurements from which it is possible to determine the different mental activity kinds. In this case, the chosen measurement is the mean of the wavelet coefficients in the principal frequency bands of the brainwaves.

Figure 4.1 illustrates the feature extraction of the wavelet coefficients in the five regions correspondent to the brainwaves frequency ranges, where X_μ is the feature vector of the means of the wavelet coefficients.

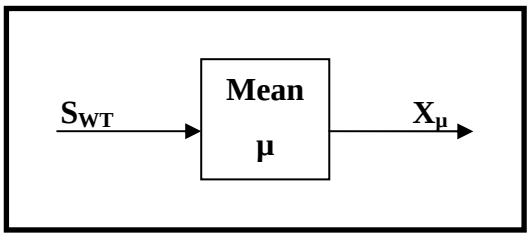

Figure 4.1 – Feature extraction of the wavelet coefficients.

4.4 Pattern Recognition

Pattern recognition consists in determining an algorithm to classify the signal's features according to the corresponding mental task. A probabilistic neural network is used as classifier, obtaining a high hit rate in comparison with a MLP when were tested; the classifier must be able to recognize five different mental activities.

To train the neural network, 500 trials are taken where the user is asked to carry out 100 trials of the chosen mental activities: motor imagery of the forefinger movement to the right side (RM), motor imagery of the forefinger movement to the left side (LM), 3D rotation of a cube (CR), arithmetic operation of subtraction (AS), and the mental state of relax (RX).

After computing the mean of the wavelet coefficients, the dimension of the feature vector is 50, five regions after the wavelet transform and ten electrodes; using the knowledge of the specialization of the brain activity and the position of

the electrodes it is possible to discard the electrodes Fp1, Fp2, P3 and P4, achieving a reduction of the dimensionality to 30. Then, the brain activity principal concentration is observed in the delta band [0 – 4 Hz], reducing the dimensionality to 6. Validation of the classifier allows discarding the electrodes C4 and Pz, then the final dimension of the feature vector is 4.

The reduction of the dimensionality eases the training and application of the neural network. Therefore, the processing time is reduced too, which is an important requirement for applications in real time (see Fig. 4.2, where MA is the recognized mental activity).

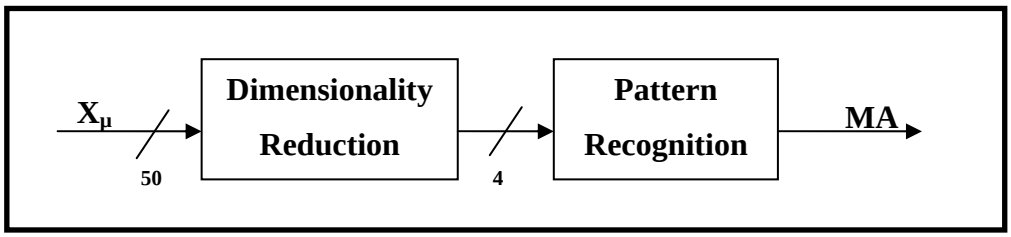

Figure 4.2 – Pattern recognition of the five mental activities.

The trials with their reduced feature vector are divided in the following way: 80% of the trials are taken for the training data and 20% for the validation data. Cross-validation is applied in the same way that in the artifact detection, to determine the neural network with better performance in the classification (Haykin, 2005).

Table 7 shows the confusion matrix from the classification in the stage of validation of the neural network. The obtained hit rate is 83%.

Table 7 – Confusion Matrix of the Classification of the Mental Activities with a PNN neural network. RM: Motor imagery of the movement of the forefinger to the right side. LM: Motor imagery of the movement of the forefinger to the left side. CR: 3D Rotation of a cube. AS: Arithmetic operation of subtraction. RX: Relax.

	RM	**LM**	**CR**	**AS**	**RX**
RM	16	4	0	0	0
LM	0	15	5	0	0
CR	1	5	14	0	0
AS	1	1	0	18	0
RX	0	0	0	0	20

4.5

4.6
Summary and Conclusions

This chapter described the data processing procedure, divided into two stages. The first stage is the feature recognition, where the chosen measurement is based on the references that extract some characteristic of the behavior of the signal in the time-frequency domain. The feature vector obtained must be reduced to ease the calculation and to decrease the processing time.

The obtained hit rate of 83% for the PNN was better than the MLP neural network, which obtained 63%. Table 7 shows the confusion matrix, with a relatively low number of misclassifications with respect to the total of the trials of the validation data (100).

Figure 4.3 illustrates the block diagram of the processing of the digitalized EEG signal. The MA can be used for whatever application; in this work, the activation of the movements of a mobile robot.

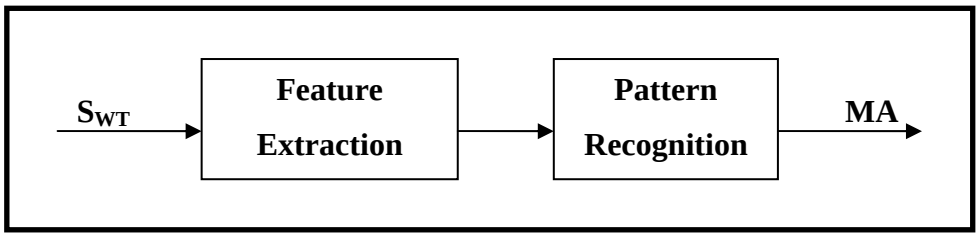

Figure 4.3 – Block diagram of the processing of the digitalized EEG signal.

The experimental results with a mobile robot are presented in the next chapter.

5
APPLICATION

5.1
Introduction

In the previous chapters, the methodology for each one of the subsystems of the BCI was described in detail. The EEG signals free of artifacts are processed to extract features that can be useful for the recognition of mental activities.

The stages of training and application of the BCI must be automatic processes; the development of a graphic interface that can link all the subsystems in different programming environments, and interact with the available hardware is necessary.

The graphic interface is developed in the programming environment Visual C#, adding libraries to run routines in Matlab to control data acquisition through the "CompactDAQ" and to send commands for the mobile robot by the radiofrequency (RF) interface. This interface offers to the user a friendly environment to develop the skill of controlling his/her brain activity while the system can adapt with him/her.

The validation of the BCI is made through an application which consists on the activation of the movements of a mobile robot associating the mental activities to commands that can be sent to the robot by the radiofrequency interface. This application is tested with five users, evaluating the performance of the BCI with different measurements that explain the accuracy and speed of the integrated system.

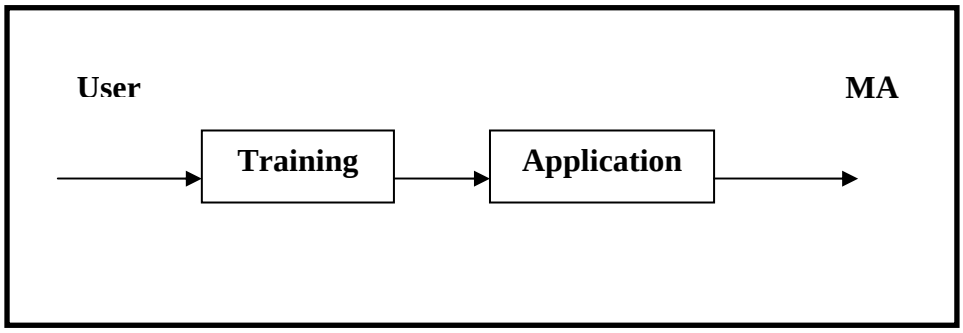

Figure 5.1 – Block diagram of the sequence of stages in the application.

5.2 Training Protocol

The training protocol is described as a sequence of three stages; see Fig. 5.2, which are described next.

The first stage consists on the artifact detection through the training of two neural networks, which detect the occurrence of ocular and muscular artifacts; the procedure in this stage is described in detail in the section 3.3.6.

The second stage consists on the mental activity recognition through the training of a PNN, which is achieved classifying the five kinds of mental activities; the procedure in this stage is described in detail in the section 4.4.

The third stage consists on the mutual adaptation between the system and the user, providing to the user visual feedback (biofeedback). In such feedback, the mental activity to be developed is shown randomly on the screen. If the classifier point out a different mental activity; then, the acquired signal is discarded.

This procedure is repeated so much as to complete 10 trials of each kind of mental activity, the trials resulted are added to the PNN neural network. The obtained data in the section 4.4 is used to validate this procedure. 10% of the trials are taken for the stage of the mutual adaptation, while another 10% of the trials are taken for validation data.

The hit rate of the network of the second stage is 82%, while that the hit rate of the network of the third stage is 92%.

Figure 5.2 – Training protocol applied to a user.

5.3 Graphical Interface

The graphical interface is developed in the programming environment Visual C# adding libraries to run routines in MATLAB to control the data acquisition through the “CompactDAQ” hardware and to send commands for the mobile robot by the radiofrequency (RF) interface.

This interface offers to the user a friendly environment to develop the skill of controlling his/her brain activity.

The interface has four options: Acquisition option, which allows continuous data acquisition; Control RF, which sends commands through radiofrequency to a receiver device; Training option, which accomplishes the training procedure in its three stages (see Fig. 5.3); and Application option, which applies the obtained results in the training procedure to activate a mobile robot through radiofrequency (see Fig. 5.4).

The application option loads a file containing the classification data according to a specific user trained previously. It recognizes the kind of mental activity from the user, associating each classification with an established command to the robot.

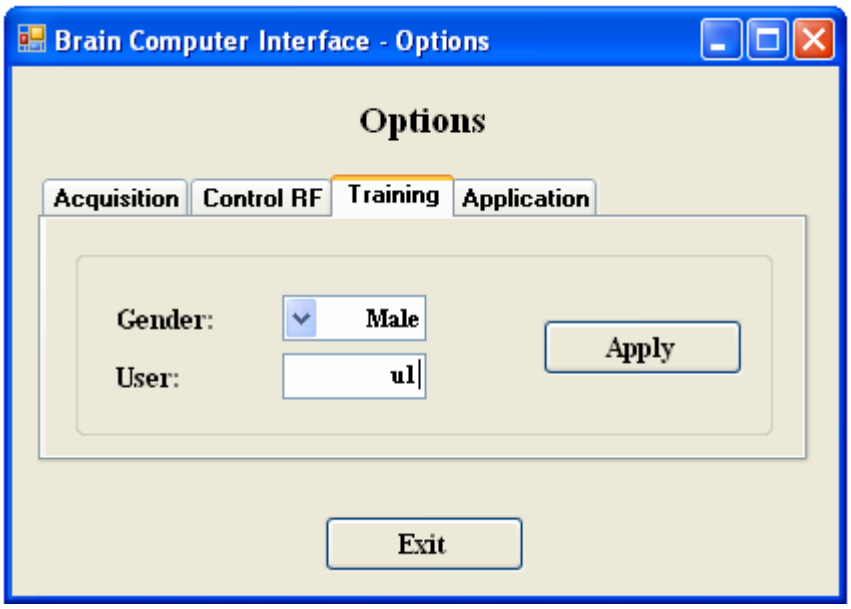

Figure 5.3 – Training option of the interface.

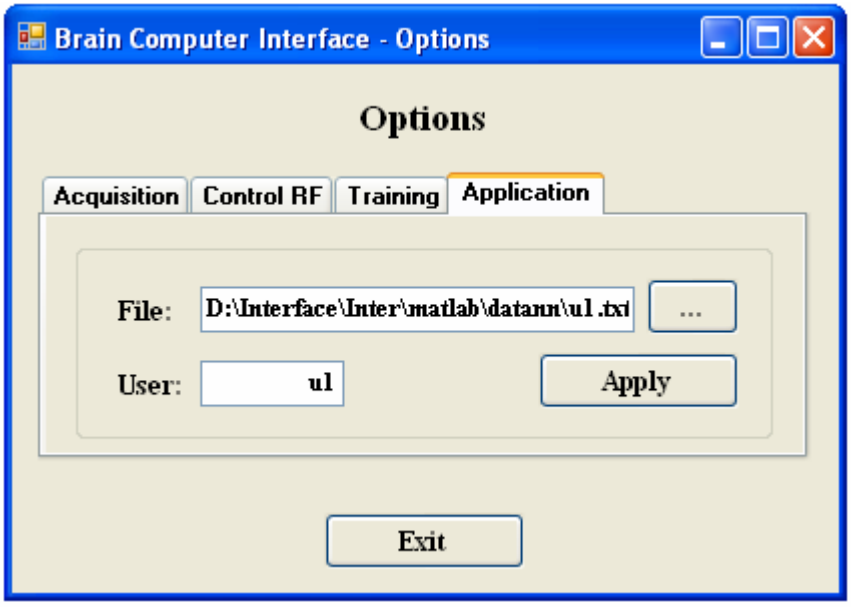

Figure 5.4 – Application option of the interface.

5.4 Application

To validate the proposed methodology, the developed BCI is applied to a 120 pound mobile robot. The chosen mobile robot, named *"Touro"* (see Fig. 5.5), were available at PUC-Rio's Robotic Laboratory, setup to respond to RF commands, therefore no further development was necessary. In addition, this system is analogous to a powered wheelchair, one of the possible applications of the BCI: it is driven by only two active wheels (see Fig. 5.6) using "tank steering", and it has enough torque to carry an adult.

Figure 5.5 – Mobile robot *"Touro"* of the application.

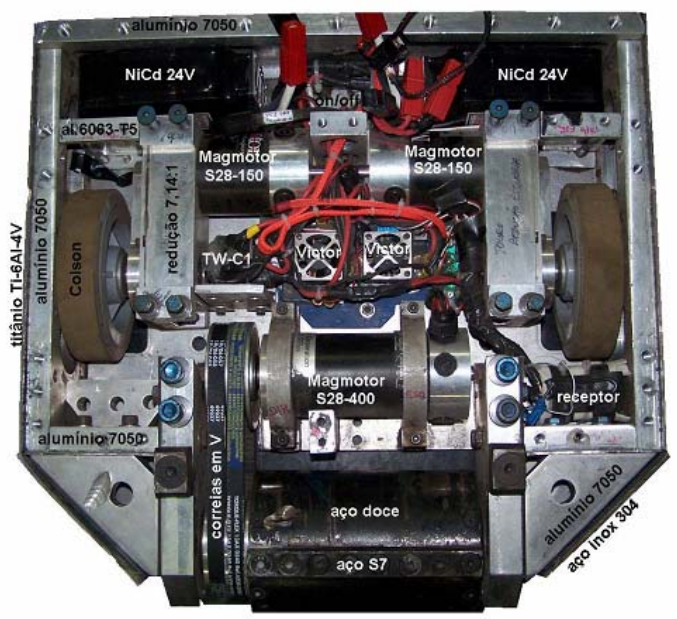

Figure 5.6 – Differential traction configuration of the mobile robot *"Touro"*.

The BCI commands are translated to five different commands: turn right, turn left, move forward, move backward, and stop.

The Figure 5.7 shows the application of the BCI.

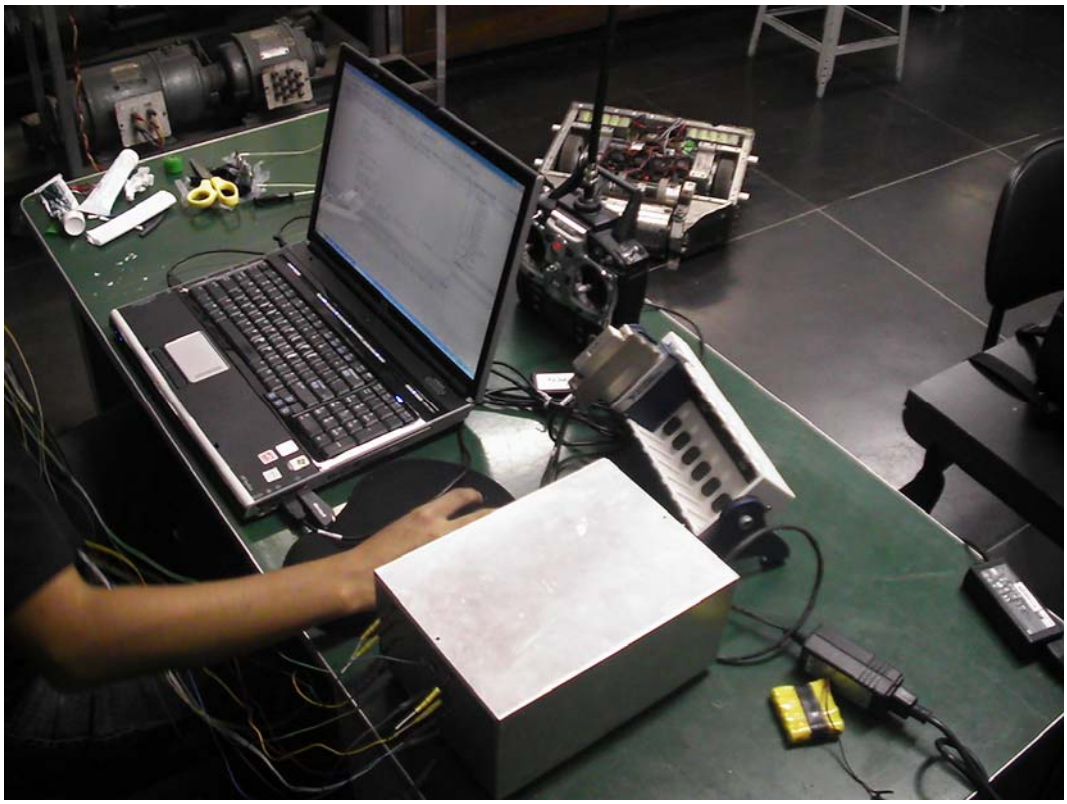

Figure 5.7 – Application of the brain computer interface.

The application to activate the robot is contained in the graphical interface, each processing of a command take approximately 2.5 seconds; therefore, the transmission rate is 25 commands/minute. The hit rate obtained of the application is 40 %.

The Table 8 shows the comparison between mental activities and classifiers's output resulting of the application test.

Table 8 – Comparison between mental activities and classifier's output.

Mental activity	**Classifier's output**
RM	RM
LM	AS
CR	RM
AS	RM
RX	RM
RX	RX
CR	CR
AS	RM
LM	LM
RM	RX

5.5 Summary and Conclusions

This chapter described the training protocol, the graphical interface and the application.

The training protocol take approximately three hours, the computer used in this test is a notebook with processor AMD Turion64, 1.8 GHz and 1GB of RAM.

The graphical interface was programmed to accomplish the three stages of the training automatically and sequentially.

The mental activities classifier must be improved to increase the hit rate of the classification.

The block diagram of the integrated system can be seen in the Fig. 5.8.

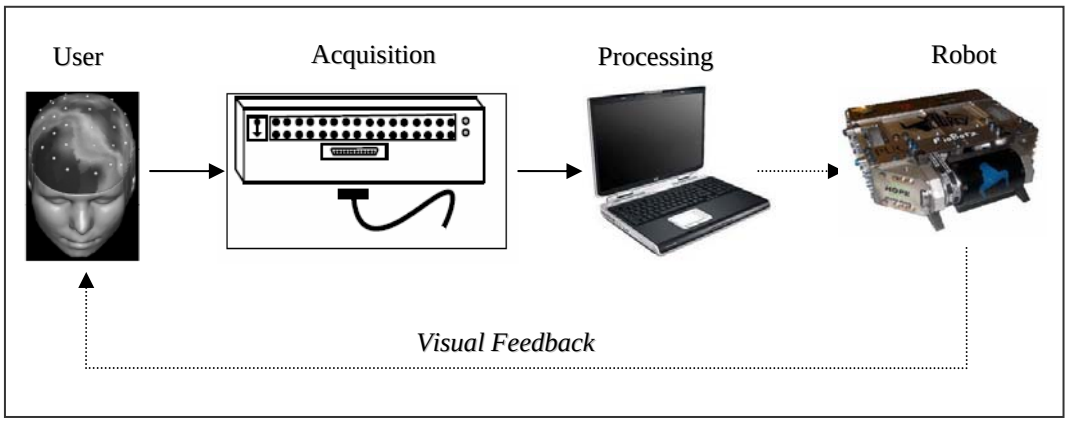

Figure 5.8 – The block diagram of the integrated system.

6
CONCLUSIONS

The objectives of this dissertation were to:

- Design and implement an EEG signal acquisition system,
- Design and develop an asynchronous operant conditioning based BCI system, which carries out a training procedure based in mutual adaptation between the system and the user, through the adjustment of the system parameters and the feedback to the user.
- Ensure that the BCI is free of the influence of signals of similar procedence such as ocular and muscular artifacts.
- Establish efficient evaluation schemes and training protocols.

6.1
Summary of achievements

The major achievements in this work can be summarized as follows.

- A 10-channel EEG signal acquisition system was implemented to develop the BCI.
- An asynchronous operant conditioning BCI was developed, which operates with five mental activities in the activation framework of a mobile robot, the BCI sends commands each 2.5 seconds.
- An efficient algorithm to detect ocular and muscular artifacts was developed based on the training and composition of two neural networks. The parameters of this artifact detection system were set during a first training stage.
- It was found that the selected features to train the neural networks in the artifact detection stage and the recognition stage represent suitably the behavior of the EEG signals in the frequency-time domain in each band of the EEG analysis.

6.2 Future directions

The BCI research depends of the development of neuroscience, technology and computational methods necessary for an efficient performance of the system. The follow proposals are possible extensions of this work.

- The implemented EEG signal acquisition system can be improved, if the design contemplates surface electronic components, reducing the dimensions and protecting the circuits from noise influence.
- The mental activities were chosen according to hemispheric brain specialization. The kinds of mental activity defined to train the classifiers, limiting the user to only them. The users could select, in future versions, the kind of mental activity with which they have more predisposition to operate the BCI.
- The system implemented must be tested according to safety norms to guarantee the protection of the user, the recommended norm is the norm IEC 60601-1 (Medical electrical equipment – Part 1: General requirements for basic safety and essential performance).
- The BCI can evolve to a Brain Machine Interface (BMI), which is implemented in an embedded system. The BMI will offer portability and improved user friendliness.

REFERENCES

Anderson, C.W. Effects of variations in neural network topology and output averaging on the discrimination of mental tasks from spontaneous EEG, Journal of Intelligent Systems, 7:165–190.1997.

Akay, M. Wavelets applications in medicine. Spectrum, May 1997, pp. 50-57.

Allanson, J. Upporting the Development of Electrophysiologically Interactive Computer Systems, PhD thesis, Lancaster University, 2000.

Babiloni, F.; Cincotti, F.; Lazzarini, L.; Millan, J.; Mourino, J.; Varsta, M.; Heikkonen, J.; Bianchi, L.; Marciani, M. G. Linear Classification of Low-Resolution EEG Patterns Produced by Imagined Hand Movements, IEEE Transactions Rehabilitation Engineering, 8(2):186–188, 2000.

Barea, R. Electroencefalografía, Instrumentación Biomédica. Departamento Electrónica. Universidad Alcalá. Tema5, 2002.

Barreto, A. B.; Scargle, S. D.; Adjouadi M. A practical emg-based human-computer interface for users with motor disabilities, Journal of Rehabilitation Research and Development, 37(1):53–63, 2000.

Bayliss, J. D. A Flexible Brain-Computer Interface, PhD thesis, Department of Computer Science University of Rochester, 2001.

Bayliss, J. D. Use of the Evoked Potential P3 Component for Control in a Virtual Apartment, IEEE Transactions Rehabilitation Engineering, 11(2):113–116, June 2003.

Benning, M.; Boyd, S.; Cochrane, A.; Uddenberg, D. The Experimental Portable EEG/EMG Amplifier, ELEC 499A Report, University of Victoria, Faculty of Engineering, August 2003.

Birbaumer, N. A spelling device for the paralysed, Nature, 398:297–298, 1999.

Birbaumer, N.; Kubler, A.; Ghanayim, N.; Hinterberger, T.; Perelmouter, J.; Kaiser, J.; Iversen, I.; Kotchoubey, B.; Neumann, N.; Flor, H. The Thought Translation Device (TTD) for Completely Paralyzed Patients, IEEE Transactions on Neural Systems and Rehabilitation Engineering, 8:190–193, 2000.

Birbaumer, N.; Hinterberger, T.; Kubler, A.; Neumann, N. The Thought Translation Device (TTD): Neuro behavioral Mechanisms and Clinical Outcome, IEEE Transactions on Neural Systems and Rehabilitation Engineering, 11(2):120–123, 2003.

Bourhis, G.; Horn, O.; Habert O.; Pruski, A. An Autonomous Vehicle for People with Motor Disabilities, IEEE Robotics & Automation Magazine, vol. 8, no. 1, pp 20-28, March 2001.

Calhoun, G. L.; McMillan, G. R.; Ingle, D. F.; Middendorf, M. S. Eeg-based control: Neurologic mechanisms of steady-state self-regulation, Technical Report AL/CF-TR-1997-0047, Wright-Patterson Air Force Base, 1997.

Cheng, M.; Gao, X.; Gao, S.; Xu, D. Design and Implementation of a Brain-Computer Interface With High Transfer Rates, IEEE Transactions on Biomedical Engineering, 49(10):1181–1186, 2002.

Cotrina, A. R. Sistemas de adquisición y procesamiento de las señales del cerebro, Informe de suficiencia para optar el título profesional de ingeniero electronico, Departamento de Ingeniería Eléctrica y Electrónica, Universidad nacional de Ingeniería, 2003.

Delorme, A.; Jung, T.; Sejnowski, T.; Makeig, S. Improved rejection of artifacts from EEG data using high-order statistics and independent component analysis. Neuroimage, 2005.

Devulapalli, S. Nonlinear principal component analysis and classification of EEG during mental tasks, Master’s thesis, Department of Computer Science, Colorado State Univ., 1996.

Donchin, E.; Smith, D. B. The contingent negative variation and the late positive wave of the average evoked potential, Electroencephalography and Clinical Neurophysiology, 29:201–203, 1970.

Donchin, E.; Spencer, K. M.; Wijesinghe R. S. The mental prosthesis: Assessing the speed of a p300-based brain-computer interface, IEEE Transactions on Rehabilitation Engineering, 8:174–179, 2000.

Erdogmus, D.; Hild, K. E. II; Principe, J. C. Blind source separation using Renyis marginal entropies. Neurocomputing, v. 49, pp. 25-38, 2002.

Evans, J. R.; Abarbanel, A. Introduction to Quantitative EEG and Neurofeedback, Academic Press, 1999.

Farwell, L. A.; Donchin, E. Talking of the top of your head: A mental prosthesis utilizing event related brain potentials, Electroencephalography and Clinical Neurophysiology, (70):510–523, 1998.

Findji, F.; Catani, P.; Liard, C. Topographical distribution of delta rhythms during sleep: Evolution with age, Electroencephalography and Clinical Neurophysiology, 51(6):659–665, 1981.

Freeman, W. J. Induced rhythms in the brain, chapter Predictions on neocortical dynamics derived from studies in paleocortex, Springer Verlag, pp. 183–199, 1992.

Galin, D.; Ornstein, R. F. Lateral specialization of cognitive mode: An EEG study, Psycophysiology, 9:412–418, 1972.

Galin, D.; Ornstein, R. F. Human Behavior and Brain Function, chapter Hemispheric Specialization and the Duality of Consciousness, pp. 3–23, Thomas Books, 1975.

Gao, X.; Xu, D.; Cheng, M.; Gao, S. A BCI-based Environmental Controller for the Motion Disabled, IEEE Transactions on Neural Systems and Rehabilitation Engineering, 11(2):137–140, June 2003.

Garcia, G. N.; Ebrahimi, T.; Vesin, J. M. Support vector EEG classification in the fourier and time-frequency correlation domains, Proceedings of the First IEEE EMBS Conference on Neural Engineering, pp. 591–594, March 2003.

Garcia, G. N. Direct brain-computer communication through scalp recorded EEG signals, Doctor's thesis, Department of Electricity, Ecole Polytechnique Fédérale de Lausanne, Lausanne, 2004.

Garcia, G. N.; Hoffmann, U.; Ebrahimi, T.; Vesin. J. M. Direct Brain-Computer Communication through EEG Signals, IEEE EMBS Book Series on Neural Engineering, 2004.

Gevins, A.; Smith, M.; McEvoy, L.; Leong, H.; Le, J. Electroencephalographic imaging of higher brain function, Philisophical Transactions of the Royal Society, (354):1125–1134, 1999.

Ghandeharion H.; Erfanian A. A fully automatic method for ocular artifact suppression from EEG data using wavelet transform and independent component analysis. Proceedings of the 28th IEEE EMBS Annual Internatonal Conference, pp. 5265-5268, 2004.

Griffiths, D.; Nelo; Peters, J.; Robinson, A.; Spaar J.; Vilnai, Y. The modular EEG design 2002, OpenEGG Community, available in: <http://openeeg.sourceforge.net/>, access on 31th september, 2005.

Haykin, S.; Neural networks: A comprehensive foundation, Prentice Hall, second edition, 1998.

Harner, P. F.; Sannit, T. A review of the International Ten-Twenty system of electrode placement, Grass Instruments Company, 1974.

Hirano, K.; Nishimura, S.; Mitra, S. K. Design of Digital Notch Filters, IEEE Transactions on Circuits and Systems, 22(7): 964–970, 1974.

Huggins, J.E.; Levine, S.P.; BeMent, S.L.; Kushwaha, R.K.; Schuh, L. A.; Rohde, M. M.; Ross, D.A. Detection of event related potentials for development of a direct brain interface, Journal of Clinical Neurophysiology, 16:448–455, 1999.

Inuso, G.; La Floresta F.; Mammone; Nadia; Morabito, F. C. Brain activity investigation by EEG processing: wavelet analysis, kurtosis and Renyi's entropy for artifact detection, Proceedings of the 2007 International Conference on Information Acquisition, Jeju City, pp. 195–200, 2007.

Jasper, H.H.; Penfield, W; Electrocorticograms in man: effect of the voluntary movement upon the electrical activity of the precentral gyrus, Arch. Psychiat. Z., Neurol., 183:163174, 1949.

Jahankhani, P.; Kodogiannis, V.; Revett, K. EEG signal classification using wavelet feature extraction and neural networks. Jhon Vincent Atanasoff 2006 International Symposium on Modern Computing, pp. 120-124, 2006.

Jeannerod, M. J. Mental imagery in the motor context, Neuropsychologia, 33(11):1419–1432, 1995.

Kalcher, J. Graz brain-computer interface II, Med. & Biol. Eng. & Comput., 34:382–388. 1996.

Lee, J. C.; Tan D. S. Using a Low-Cost Electroencephalograph for Task Classification in HCI Research The nineteenth annual ACM Symposium on User Interface Software and Technology, October 15-18, Montreux, Switzerland, pp. 81-90, 2006.

Lopes da Silva, F. H. Neural mechanisms underlying brain waves: from neural membranes to networks. Electroencephalography and Clinical Neurophysiology, 79:81–93, 1991.

Koenig, T.; Kochi, K.; Lehmann, D. Event-related electric microstates of the brain differ between words with visual and abstract meaning, Electroencephalography and Clinical Neurophysiology, 106(6):535–546, 1998.

Makeig, S.; Jung, T.-P.; Bell, A. J.; Ghahremani, D.; Sejnowski, T. J. Blind Separation of Auditory Event-related Brain Responses into Independent Components, Proceedings of the National Academy of Sciences of the United States of America, 94:10979–10984,1997.

Middendorf, M.S.; McMillan, G. R.; Calhoun, G. L.; Jones, K. S. Brain-Computer Interfaces Based on the Steady-State Visual-Evoked Response, IEEE Transactions on Rehabilitation Engineering, 8:211–214, 2000.

Millan, J. d. R. Brain-Computer Interfaces, Handbook of Brain Theory and Neural Networks, Second edition, Cambridge, MA, The MIT Press, 2002.

Millán, J. del R.; Mouriño, J.; Franzé M., Cincotti, F., Varsta, M., Heikkonen, J.; Babiloni, F. A local neural classifier for the recognition of EEG patterns associated to mental tasks, IEEE Trans. on Neural Networks, 11:678–686, 2002.

Millan, J. del R.; Mourino, J. Asynchronous BCI and local neural classifiers: an overview of the adaptive brain interface project, IEEE Transactions on Neural Systems and Rehabilitation Engineering, 11(2):159–161, 2003.

Millán, J. d. R.; Renkens, F.; Mouriño, J.; Gerstner, W. Noninvasive Brain-Actuated Control of a Mobile Robot by Human EEG, IEEE Transactions on Biomedical Engineering, vol. 51, no. 6, pp 1026-1033, June 2004.

Miller, R. Cortico-hippocampal interplay and the representation of contexts of the brain, Springer Verlag, 1991.

Muller, K. R.; Anderson, C. W.; Birch, G. E. Linear and Nonlinear Methods for Brain-Computer Interfaces, IEEE Transactions on Neural Systems and Rehabilitation Engineering, vol. 11, no. 2, pp. 165–169, 2003.

National Instruments, Build Your Own NI CompactDAQ System, available in <http://ohm.ni.com/advisors/compactdaq>, access on 2nd july, 2007.

Nikolaev, A. R.; Anokhin, A. P. Eeg frequency ranges during perception and mental Rotation of two and three dimentional objects, Neuroscience and Behavioral Physiology, 6(28):670–677, 1998.

Obermaier, B.; Müller, G.; Pfurtscheller, G., 'Virtual Keyboard' controlled by spontaneous EEG activity, Proceedings of the International Conference on Artificial Neural Networks, Heidelberg: Springer-Verlag. 2001.

Golden, R. M. Digital filters by sampled-data transformation, IEEE Transactions Audio and Electroacustics, AU-16:321–329, 1968.

Obermaier, B.; Neuper, C.; Guger, C.; Pfurtscheller, G. Information Transfer Rate in a Five-Classes Brain Computer Interface, IEEE Transactions on Neural Systems and Rehabilitation Engineering, 9(3):283–288, 2001.

Overton D. A.; C. Shagass. Distribution of eye movement and eye blink potentials over the scalp, Electroencephalography and Clinical Neurophysiology, n. 27, pp. 546, 1969.

Pascual-Marqui, R. D.; Michel, C.M.; Lehmann, D. Segmentation of brain electrical activity into microstates: model estimation and validation, IEEE Transactions on Biomedical Engineering, vol. 42, no. 7, pp. 658–665, 1995.

Perelmouter, J.; Birbaumer, N. A Binary Spelling Interface with Random Errors, IEEE Transactions on Rehabilitation Engineering, 8(2):227–232, 2000.

Pertence A. Amplificadores operacionais e filtros ativos, McGraw – Hill, 1988.

Pfurtscheller and, G.; Aranibar, A. Event-related cortical desynchronization detected by power measurements of scalp EEG, Electroencephalography and Clinical Neurophysiology, 42:817–826, 1977.

Pfurtscheller and, G.; Neuper, C. Motor Imagery and Direct Brain-Computer Communication, Proceedings IEEE, 89:1123–1134, 2001.

Pfurtscheller, G.; Neuper, C.; Muller, G. R.; Obermaier, B.; Krausz, G.; Schlogl, A.; Scherer, R.; Graimann, B.; Keinrath, C.; Skliris, D.; Wortz, M.; Supp, G.; Schrank, C. Graz-bci: State of the Art and Clinical Applications, IEEE Transactions on Neural Systems and Rehabilitation Engineering, 11(2):177–180, 2003.

Proakis, J. G.; Manolakis, D. G. Digital Signal Processing, Prentice Hall, Inc. 1996.

Robbins, J. A Symphony in the Brain, Atlantic Monthly Press, 2000.

Rockstroh, B.; Birbaumer, N.; Elbert, T.; Lutzenberger, W. Operant control of EEG and event-related and slow brain potentials, Biofeedback and Self Regulation, 9:139160, 1984.

Rotenberg, V. S.; Arshavsky, V. V. Right and left brain hemispheres activation in the representatives of two different cultures, Homeostasis in Health & Disease, 38(2):49–57, 1997.

Singer, W. Synchronization of cortical activity and its putative role in information processing and learning, Annual Review of Physiology, 55:349–374, 1993.

Skinner, B. F. The Behavior of Organizms, NewYork: Appleton, 1938.

Sutton, S.; Braren, M.; Zubin, J.; John, E. R. Evoked correlates of stimulus uncertainty, Science, 150:1187–1188, 1965.

Sykacek, P.; Roberts, S.; Stokes, M.; Curran, E.; Gibbs, M.; Pickup. L. Probabilistic Methods in BCI Research, IEEE Transactions on Neural Systems and Rehabilitation Engineering, vol. 11, no. 2, pp. 192–195, June 2003.

Tallon-Boudry, C.; Bertrand, O.; Peronnet, F.; Pernier, J. Induced gamma-band activity during the delay of a visual short-term memory task in humans, Journal of Neuroscience, (11):4244–4254,1998.

Tecce, J. J.; Gips, J.; Olivieri, C. P.; Pok, L. J.; Consiglio M. R. Eye movement control of computer functions, International Journal of Psychophysiology, 29:319–325, 1998.

Texas Instrument Incorporated. INA114 Precision Instrumentation Amplifier Datasheet, 14p, .2003.

Thorpe, S.; Fize, D.; Marlot, C. Speed of processing in the human visual system, Nature, pp. 520–522,1996.

Utall, W. R. The War Between Mentalism and Behaviorism: On the Accessibility of Mental Processes, NJ:Erlbaum, 1999.

Van de Velde, M.; Van Erp, G.; Cluitmans, P. J. M. Detection of muscle artifact in the normal human awake EEG. Electroencephalography and Clinical Neurophysiology, 107(2):149–158, April1998.

Vaughan, T. M.; Heetderks, W. J.; Trejo, L. J.; Rymer, W. Z. Brain-Computer Interface Technology: A Review of the Second International Meeting, IEEE Transactions on Neural Systems and Rehabilitation Engineering, 11(2):94–109, June 2003.

Walter, W. G.; Cooper, R.; Aldridge, V. J.; McCallum, W. C.; Winter, A. L. Contingent negative variation: an electric sign of sensorimotor association and expectancy in the human brain, Nature, 203:380–384, 1964.

Windhorst, U.; Johansson, H. Modern Techniques in Neuroscience Research, SpringerVerlag, 1999.

Wolpaw, J.R.; McFarland, D.J. Multichannel EEG-based brain-computer communication, Electroenceph. Clin. Neurophysiol., 90:444–449. 1994.

Wolpaw, J.R.; McFarland, D. J.; Vaughan, T.M. Brain Computer Interface Research at the Wadsworth Center, IEEE Transactions on Neural Systems and Rehabilitation Engineering, 8:222–226, 2000.